POLITECNICO DI TORINO

Collegio di Ingegneria Chimica e dei Materiali

Corso di Laurea Magistrale

in Ingegneria Chimica e dei Processi Sostenibili

Tesi di Laurea Magistrale

Characterization of the deflagration parameters of the dust deriving from the processing of the olive pomace

Relatore

Prof. Luca Marmo

Correlatore

Dott. Enrico Danzi

Candidato

Mónica Andreina Silva Durán

Marzo 2019

To my dear uncle Alvaro.

For always believing in me, even when I do not believe in myself

Riassunto in italiano

Il rischio di esplosione di polveri combustibili rappresenta una minaccia costante nei processi industriali che coinvolgono materiali sotto forma di polveri. Queste esplosioni possono verificarsi quando particelle di dimensioni ridotte (inferiori ai 500μm) combustibili vengono disperse in un ambiente confinato in presenza di una sorgente innesco. Per evitare e prevenire l'esplosione di polveri nei luoghi di lavoro sono state sviluppate diverse prove esperimentali, regolate da standard a livello internazione, con lo scopo di determinare e caratterizzare la tendenza delle polveri a innescare, così come la gravità delle esplosioni che possono generare.

È noto che negli ultimi anni la produzione di olio d'oliva è aumentata nei paesi mediterranei come la Spagna, l'Italia, la Grecia e la Turchia. Tuttavia, l'estrazione dell'olio d'oliva produce enormi quantità di rifiuti e sottoprodotti che hanno un impatto ambientale. Questi materiali includono la cosiddetta "sansa d'oliva umida" e la sansa di oliva. Le relative frazioni dipendono dalla natura del delle olive e dalla tecnologia di estrazione dell'olio applicata. I due tipi di sansa di oliva contengono frammenti di nocciole, bruccia e polpa in diverse proporzioni. Differiscono nel contenuto di umidità e nella composizione chimica. Inoltre, sono derivati da diverse tecnologie di estrazione primaria e sono sottoposti a estrazioni secondarie con solventi come esano.

La sansa di oliva è interessante come fonte alternativa di combustibile. Ciò è dovuto al suo alto potere calorifico, e alla facilità di ottenere grandi quantità dall'estrazione dei processi dell'olio d'oliva.

Dalla lavorazione dell'olio d'oliva si ottiene un prodotto sotto forma di pellet, che può generare notevoli quantità di polvere, in seguito a movimentazione e urti. Pertanto, questo lavoro si è concentrato sulla determinazione dei parametri, che caratterizzano la deflagrazione della polvere di sansa di oliva. A tale scopo, è stata condotta una caratterizzazione fisica di un campione ottenuto da un processo centrifugo di estrazione dell'olio a due fasi (decanter).

L'analisi consisteva nella determinazione della distribuzione delle dimensioni delle particelle, della morfologia, del calore di combustione e del contenuto di umidità. In seguito sono stati determinati presso il Centro Sperimentale Sicurezza Industriale Atmosfere Esplosive del Politecnico di Torino, i parametri di deflagrazione: la temperatura minima di accensione di una nube di polvere (MIT), la temperatura minima di accensione di uno strato di polvere (LIT), il limite inferiore di esplosività (LEL), la massima pressione di esplosione (Pmax) e l'indice deflagrante (KSt). Inoltre, preliminarmente alle misure dei parametri deflagranti è stato condotto un test di screening di infiammabilità per stabilire se il campione di polvere fosse infiammabile o no, secondo la normativa ISO 80079-20-2: 2016.

Parametri di deflagrazione della polvere

- *Temperatura minima di accensione di una nube di polvere (MIT)*

La temperatura minima di accensione di una nube di polvere è definita dalla normativa CEI EN 50281-2-1 (1999) come la temperatura minima di una superficie calda che provochi l'innesco di una nube di polvere dispersa in aria. L'unità di misura è °C.

- *Temperatura minima di accensione di uno strato di polvere (LIT)*

La normativa CEI EN 50281-2-1 (1999) define la temperatura minima di accensione di uno strato di polvere come la temperatura minima di una superficie calda prestabilita che provochi la decomposizione e/o l'innesco di uno strato di polvere di spessore specificato, su di essa depositato. Viene misurata in °C.

- *Velocità massima di aumento della pressione di esplosione $(dP / dt)_{max}$*

Secondo la normativa EN 14034-2, 2006+ A1:2011, la velcoità massima di aumento della pressione è Il tasso massimo di aumento di pressione per unità di tempo durante un'esplosione in un recipiente chiuso. L'unità di musira è bar s^{-1}.

- *Indice di deflagrazione K_{St}*

L'indice K_{St} [bar m / s] è un parametro importante che caratterizza la violenza dell'esplosione e deriva dal valore $(dP / dt)_{max}$. La contrazione "St" deriva dalla parola tedesca "staub", che significa "polvere".

Tabella 1: Classi di pericolo per esplosioni di polveri, da Cesana, G., et al., (2016).

Intervalli	Classe	Esplosività
$K_{St}=0$	St_0	Non esplosivo
$0 < K_{St} < 200$	St_1	Debole
$200 < K_{St} < 300$	St_2	Forte
$300 < K_{St}$	St_3	Molto Forte

Il valore K_{St} è direttamente correlato alla velocità massima di aumento della pressione (dP/dt) secondo la "legge della radice cubica" (equazione 1.1). Bartknecht (1971, 1978) ha proposto questa correlazione.

$$K_{St} = \left(\frac{dP}{dt}\right)_{max} \cdot V^{1/3} \quad (1.1)$$

V corrisponde al volume della camera di esplosione.

$\left(\frac{dP}{dt}\right)_{max}$: il tasso massimo di aumento della pressione (bar/s).

- *Pressione massima di esplosione P_{max}*

La massima pressione di esplosione (P_{max}) è il valore massimo della sovrapressione La massima pressione di esplosione (Pmax) è il valore massimo della sovrapressione derivata da un'esplosione in un recipiente chiuso, come definito dallo standard UNI EN 14034-1:2011. È determinato da test su un intervallo di concentrazioni di polvere. L'unità di misura è bar (g).

- *Limite inferiore di esplosività (LEL)*

La normativa EN 14034-3 (2006) define il LEL come la concentrazione più bassa della sostanza combustibile nell'aria che favorisce la propagazione della fiamma. Viene misurata in °C.

Materiali

I campioni utilizzati nelle diverse prove sono stati ottenuti da una macinazione (con mulino a lame) di un campione di sansa di oliva. Questo campione proveniva da un processo di centrifugazione a due fasi ed è stato sottoposto all'estrazione d'olio.
Dal materiale polverizzato, per l'analisi si sono stati estratti le frazioni tra 1000 e 500 µm, 500 e 250 µm, <250µm e <75µm.

Esperimenti

1. Caratterizzazione preliminare

Come parte della determinazione della distribuzione delle dimensioni delle particelle (PSD), il campione è stato setacciato. È stato utilizzato un gruppo di setacci verticali: 500 μm (ASTM nº 35), 250 μm (ASTM n ° 60), 200 μm, 125 μm (ASTM nº 120), 75 μm (ASTM nº 200), 63 μm (ASTM nº 230) e 32 μm (ASTM nº 450). La distribuzione delle dimensioni delle particelle è stata ottenuta pesando la quantità residua di polvere su ciascun setaccio.

La tecnica di diffrazione laser è stata applicata utilizzando un granulometro laser (Malvern Mastersizer E100), secondo la norma ISO 13320: 2009. L'intervallo di misurazione è compresso fra 0,01-1000 μm.

Il campione di polvere è stato caratterizzato utilizzando una microscopia elettronica con un sistema di EDX FEI-Ispect S, colonna E-SEM W con un filamento di tungsteno e una sonda a raggi X (EDX) disperdente energia. È stato applicato un livello di ingrandimento di 500 X, 200X, 3,00 KX, 10,00 KX, 15,00 KX, 20,00 KX e 50,00 KX.

La percentuale di umidità relativa è stata determinata pesando una quantità del campione in polvere. Successivamente, è stato introdotto in una stufa da laboratorio a 65 ° C per 5 ore. Infine, è stato lasciato a raffreddare in un contenitore di vetro essiccato con gel di silice, che consente il raffreddamento mantenendo l'umidità costante in un breve periodo. Infine, il campione è stato pesato.

La misurazione del potere calorifico è stata effettuata in una bomba calorimetrica a volume costante, secondo la norma ISO 1716: 2018.

2. Test di Screening

Il test di screening è costituito da quattro test diversi, suddivisi in due categorie, le prove a temperatura ambiente e le prove ad alta temperatura.

1. I test della temperatura ambiente si svolgono in:

    1.1 Accensione di polvere nel test con il tubo di Hartmann - arco continuo

    1.2 Accensione a polvere nel test con il filo caldo nel tubo di Hartmann

2. I test ad alta temperatura sono:

    2.1 Autoignizione de una nube di polvere nel forno GG

    2.2 Autoignizione di uno strato di polvere su piastra riscaldante

In base al comportamento della polvere nei test, è possibile stabilire una classificazione. In caso di accensione in una qualsiasi delle prove nel tubo di Hartmann, la polvere viene classificata come "esplosiva a temperatura ambiente". Se il campione di polvere si innesca durante i test ad alta temperatura, il campione viene classificato come "esplosiva ad alta temperatura". Altrimenti, se il campione di polvere non viene innescato in nessun test, viene classificato come "non esplosivo".

In caso di mancata accensione nel test della temperatura ambiente 1.1, il test passa alla successiva fonte di innesco (più energetica, cioè il filo caldo). Allo stesso modo, se la polvere non si accende a temperatura ambiente è necessario eseguire i test ad alta temperatura.

Successivamente, se la polvere è definita come esplosiva, per caratterizzare la violenza dell'esplosione, devono essere determinati i parametri deflagranti.

- *Tubo Hartmann- Arco continuo:*

I test sono stati eseguiti su un tubo Hartmann da 1.2 L; è fatto di vetro con dimensioni: 9 cm di diametro e 34,5 cm di altezza. La fonte di innesco è disposta all'interno del tubo nella parte inferiore.

Lo scopo del test di screening con il tubo di Hartmann è quello di analizzare la sensibilità della polvere a una fonte di accensione elettrica ad una determinata quantità di energia quando si forma la dispersione della polvere a temperatura ambiente.

I campioni di polvere sono stati testati a diverse concentrazioni: campione di massa di 0,3, 0,5 e 1 g, che hanno concentrazioni nominali rispettivamente di 250, 420 e 833 g / m^3. L'energia della scintilla utilizzata è stata 525 mJ (10μF), questo valore si riferisce al grado di sensibilità di innesco più basso e rappresenta le peggiori condizioni possibili.

Il tentativo deve essere ripetuto 10 volte per ciascuna concentrazione. Le scintille non sono considerate come un'accensione.

Nel caso in cui si osservi un'accensione, il test termina e il campione viene classificato come "Esplosivo a temperatura ambiente". Altrimenti, se non viene osservata alcuna ignizione, il campione è soggetto al test con filo caldo.

- *Tubo Hartmann - filo incandescente*

La procedura è la stessa dell'arco continuo, la differenza consiste nell'accensione, mentre un filo in lega di ferro (Constantana) sostituisce gli elettrodi. Viene passata una corrente elettrica continua di 13,1 A e 11,8 V (cioè una potenza di circa 150 W), ed è sufficiente a rendere incandescente il filo e raggiungere una temperatura superficiale del filo di circa 800 ° C. Le dimensioni del filamento sono 27 cm di lunghezza, 0,6 mm di diametro ed è avvolto in sei spirali.

I criteri di innesco sono gli dal test ad arco continuo.

- *Autoignizione delle nuvole di polvere nel forno de Godbert-Greenwald*

Il forno Godbert-Greenwald ha una geometria cilindrica disposta verticalmente con un diametro esterno pari a 250 mm. La struttura esterna è realizzata in acciaio inossidabile. All'interno, ha un tubo aperto all'atmosfera nella parte inferiore ed è ricoperto di silice. Il tubo interno ha un diametro di 36 mm, circondato da una resistenza metallica che lo riscalda. Inoltre, l'estremità superiore è collegata al supporto per la polvere attraverso un adattatore di vetro. Il forno è progettato per resistere a temperature fino a 1000 ° C.

La polvere viene dispersa all'interno del forno attraverso un impulso di aria compressa proveniente da un serbatoio e poi cade per gravità nella parte inferiore.

Questo test consente di verificare se il campione di polvere può essere acceso o meno quando viene esposto ad un ambiente ad alta temperatura. Nello specifico, l'analisi è stata effettuata a 800 ° C, come stabilito dalla ISO 890079-20-2: 2016.

Diverse concentrazioni di polvere vengono testate nel forno, ovvero 0,1, 0,3 e 0,5 g di campione di polvere, applicando una sovrappressione di circa 0,3 bar nella camera del campione. Il test è stato eseguito fino a quando è stata osservata un'accensione della polvere o dieci tentativi senza accensione prima di classificare il campione.

3. Temperatura minima di accensione di una nuve di polvere (MIT)

Come per il test di screening nel forno GG, il campione di polvere è stato testato a diverse concentrazioni (0,1 g, 0,3 g e 0,5 g), applicando la stessa sovrappressione. Si è seguita la procedura esperimentale della normativa CEI EN 50281-2-1 (1999). Il test è iniziato con una temperatura di 500 ° C e procede con un aumento di 50 ° C per ciascuna ripresa fino a quando non è stata osservata un'accensione. Una volta che la dispersione di polvere è stata accesa, la temperatura è stata ridotta di 20 ° C fino a quando non sono state eseguite dieci prove consecutive di non accensione.

4. Temperatura di accensione di uno strato di polvere (LIT)

Il LIT è stato misurato utilizzando un dispositivo di test della piastra calda di Chilworth Technologies, modello 5 mm-LIT-H. È fatto di una piastra di alluminio, sopra la quale la polvere è collocata all'interno di un anello di metallo che definisce lo strato (dimensioni 5 mm di altezza e 100 mm di diametro).

Secondo la normativa EN 14034-3 (2006), l'innesco si è verificato se:

• si misura una temperatura di 450˚C

• si misura un aumento di temperatura maggiore di 250 °C rispetto alla temperatura della piastra

• si osservano un'incandescenza o combustione visibile

Il valore finale della LIT è la minima temperature alla quale si è innescato lo strato di polvere diminuita di 10 °C.

2 Test in Sfera di Siwek 20l

Il campione di polvere è stato testato in un intervallo di concentrazione da 250 g/m^3 fino a 1000 g / m^3. Tutti i test sono stati eseguiti nella sfera Siwek da 20 l, secondo gli standard della tabella 2.

Tabella 2: Procedure per misurare i parametri deflagranti.

Parametri deflagranti	Normativa	Accenditore
$\mathbf{P_{max}}$	UNI EN 14034-1: 2004+ A1:2011	2* 5 kJ
$\mathbf{K_{St}}$	UNI EN 14034-2: 2006+ A1:2011	2* 5 kJ
LEL	UNI EN 14034-3: 2006+ A1:2011	2* 1 kJ

L'esplosione avviene in una sfera con un volume di 20 L, realizzata in acciaio inossidabile. La sfera ha una camicia d'acqua per il raffreddamento delle pareti dopo ogni esplosione. L'ingresso della polvere nella camera di esplosione avviene tramite una valvola sul fondo azionata da aria compressa. La sorgente di accensione è posizionata al centro della sfera. Nella parte superiore è chiuso con una copertura dello stesso materiale e ha due supporti per gli accenditori chimici. Una coppia di trasduttori di pressione misura l'onda di pressione di esplosione e un'unità di controllo KSEP310 registra il valore ottenuto.

- *Pressione massima P_{max} e indice di deflagrazione K_{St}*

La sfera è stata depressurizzata a -0,6 bar usando la pompa del vuoto, mentre il contenitore della polvere è stato pressurizzato a 20 bar usando il compressore. Infine, KSEP 7.0 tramite controllo da PC si apre la valvola e si innescano fli accenditori .

La fonte di accensione consisteva in due accenditori chimici con una quantità di energia pari a 5kJ ciascuno (10kJ in totale).

- *Limite inferiore di esplosività (LEL)*

Il test ha iniziato a utilizzare 10,00 g di campione di polvere, il test è stato ripetuto riducendo la massa iniziale di 5,00 g fino a quando non vi è alcuna evidenza di un'esplosione. L'energia della fonte di accensione per questo test è fornita da due accenditori da 1 kJ ciascuno (2 kJ in totale).

Tabella 3: Criterio di esplosione nella determinazione del LEL

P_{ex} [bar]	P_m [bar]	Risultato
< 0.5	< 0.2	*No esplosione*
≥ 0.5	≥ 0.2	*Esplosione*

In totale sono state definite tre serie a diversi valori di concentrazione. La media aritmetica dei valori massimi del tasso di aumento della pressione di esplosione per ciascuna serie è stata determinata per calcolare il tasso massimo di aumento della pressione di esplosione (dp/dt) massimo, utilizzando la seguente equazione.

$$\left(\frac{dP}{dt}\right)_{max} = \frac{\left(\frac{dP}{dt}\right)_{ex\,(series\,1)} + \left(\frac{dP}{dt}\right)_{ex\,(series\,2)} + \left(\frac{dP}{dt}\right)_{ex\,(series\,3)}}{3} \quad [bar \cdot s^{-1}] \text{ (3.1)}$$

La massima pressione di esplosione è stata determinata come media aritmetica della massima pressione di esplosione di ciascuna serie, come nella equazione 3.2.

$$P_{max} = \frac{P_{m\,(series\,1)} + P_{m\,(series\,2)} + P_{m\,(series\,3)}}{3} \qquad [bar] \qquad (3.2)$$

Il valore K_{St} è stato calcolato con l'equazione 3.3 (valido per la sfera da 20 l).

$$K_{St} = 0.271 \times \left(\frac{dP}{dt}\right)_{max} \quad [bar \cdot m \cdot s^{-1}] \qquad (3.3)$$

Risultati e discussioni

1 Distribuzione granulometrica (PSD)

I risultati della distribuzione delle dimensioni delle particelle (PSD) ottenuti dalla setacciatura e dalla diffrazione laser sono riportati nella tabella 4.

Tabella 4: PSD misurato mediante setacciatura e diffrattometria laser.

Setacciatura		***Diffrazione laser***					
Caratterizzazione del campione		***Undersieve < 500 µm***		***Undersieve < 250 µm***		***Undersieve < 75 µm***	
PSD [µm]	***%w***	***PSD***	***µm***	***PSD***	***µm***	***PSD***	***µm***
< 32	1.03	**d(0.1)**	97.913	**d(0.1)**	31.816	**d(0.1)**	10.631
32-63	4.94	**d(0.5)**	354.954	**d(0.5)**	173.125	**d(0.5)**	36.246
63-75	5.61	**d(0.9)**	682.648	**d(0.9)**	351.656	**d(0.9)**	82.520
75-125	8.70						
125-200	18.05						
200-250	12.24						
>250	48.59						

In base ai risultati presentati nella tabella No. 3.1, si osserva un fattore comune tra l'analisi di setacciatura e l'analisi di diffrazione laser, cioè il campione frantumato di sansa di oliva era composto principalmente da particelle con dimensioni superiori a 250 µm. L'incorerenza sui valori di d90 dell'anlisi granulometrica laser e i tagli di setacciatura deriva dalla difficoltà dello strumento laser a misurare efficacemente le dimensioni di particelle con forma non sferica (come la maggior parte di quelle ottenute da macinatura). Queste particelle allungate dovute alle vibrazioni nel processo di setacciatura potrebbero attraversare il setaccio perpendicolarmente.

Nelle figure 3.1-3.3 del Capitolo 3 sono presentate le distribuzioni cumulative delle dimensioni delle particelle di polvere e la crva differenziale delle dimensioni delle particelle di polvere, ottenute per il campione con dimensioni <500 µm, <250 µm e <75 µm.

2. Dati analitici

La polvere di sansa di oliva è stata anche caratterizzata dalla determinazione del contenuto di umidità e del potere calorifico superiore (HHV). I risultati sono riportati nella tabella 5 e 6.

Tabella 5: PCS del campione di polvere di sansa di oliva.

Campione	***Potere calorifico superiore [kcal/kg]***
500-250 µm	4594
< 250 µm	4669

La differenza tra i valori del calore di combustione determinato potrebbe essere dovuta al fatto che il potere calorifico della sansa di oliva è influenzato dal rapporto polpa/noccioli, dove la polpa ha caratteristiche energetiche superiori.

Il rapporto fra la polpa e nocciolo non è stata considerata nel presente lavoro.

Tabella 6: Contenuto di umidità delle frazioni di polvere di sansa di oliva.

Campione	*Umidità [%w]*
1000-500 µm	5.03
500-250 µm	6.39
< 250 µm	6.89
<75 µm	6.44

3 Immagini SEM

La caratterizzazione morfologica è stata ottenuta mediante immagini della microscopia elettronica a scansione nelle Fig. Da 4,4 a 4,7.

Sembra abbastanza evidente che la forma granulare predomina nella maggior parte delle particelle (Figure 1), così come le forme allungate, che assomigliano alle strutture dei trucioli di legno (Figura 1.b). D'altra parte, un ingrandimento sulla superficie delle particelle (vedi figure 2) rivela la presenza di canali all'interno delle particelle. Ciò suggerisce che la sansa di oliva è un materiale poroso elevata superficie specifica.

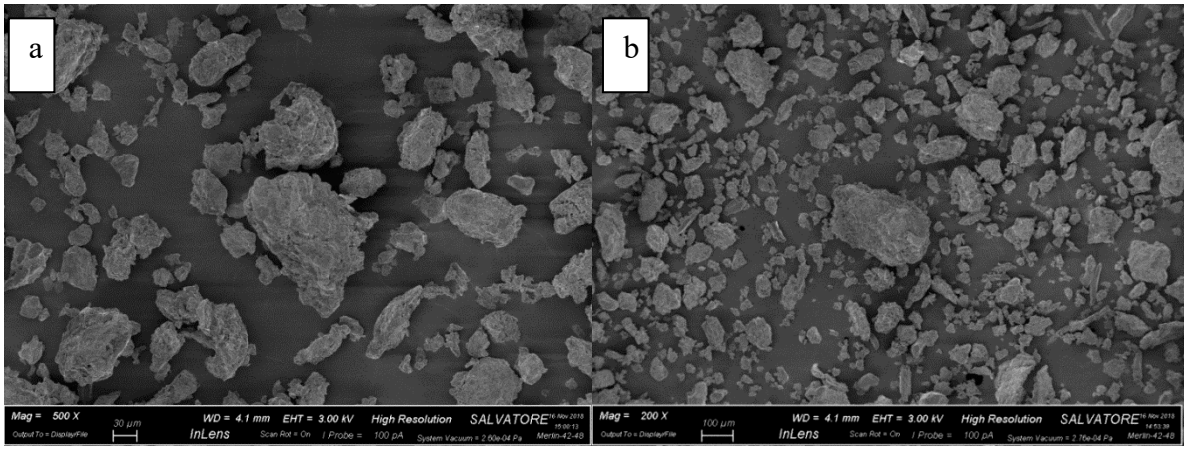

Figura 1: Immagine SEM del campione di polvere di sansa di oliva, a)500x e b)200x ingrandimento

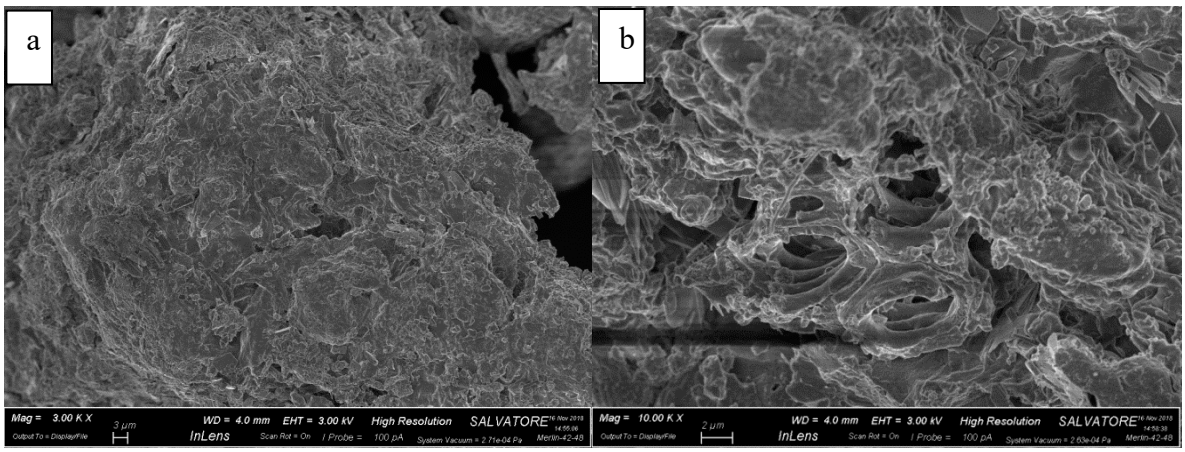

Figura 2: Immagine SEM del campione di polvere di sansa di oliva, ingrandimento a)3,00x. e b)10.00Kx.

4 Test di Screening

Il numero di inneschi/non inneschi nel test di screening sono riportaio per ciascuna frazione di dimensione del campione nella tabella 7.

Tabella 7: Risultati dei test nel tubo di Hartmann. N = nessuna accensione, P = accensione, x # indica il numero di accensione o nessuna accensione osservata.

		Tubo Hartmann		***GG forno***
Dimensioni campioni[µm]	***Massa [g]***	***Arco continuo***	***Filo Caldo***	***800˚C***
1000-500	0.3	*x*10 N	*x*10 N	P
	0.5	*x*10 N	*x*10 N	P
	1.0	*x*10 N	*x*10 N	P
< 500	0.3	*x*10 N	*x*10 N	P
	0.5	*x*10 N	*x*10 N	P
	1.0	*x*10 N	*x*10 N	P
< 75	0.3	*x*10 N	*x*10 N	P
	0.5	*x*10 N	*x*10 N	P
	1.0	*x*10 N	*x*10 N	P

La polvere è stata inizialmente testata nel tubo di Hartmann con un arco continuo. In base ai risultati presentati nella tabella 7, i campioni non si sono innescati. Pertanto, si è passata alla succesiva fonte di innesco (filo caldo). Allo stesso modo, nessuno dei campioni è stato acceso; ciò permette di classificare la polvere di sansa d'oliva come non esplosiva a temperatura ambiente.

A causa del risultato negativo delle prove su tubo di Hartmann, il test ad alta temperatura è stato eseguito nel forno GG. Per tutti i campioni si è verificato l'innesco. Questo risultato positivo per l'accensione nel forno ha permesso di classificare la polvere di sansa di oliva come esplosiva ad alte temperature. Di conseguenza, il test di screening nella piastra riscaldante non è effettuato.

5 Temperatura minima di accensione di una nube di polvere (MIT)

I valori della temperatura minima di accensione (MIT) della polvere di sansa di oliva con dimensioni comprese tra 1000-500 µm, <500 µm e <75 µm sono riportati nella tabella 8.

Tabella 8: MIT di campioni di polvere di sansa di oliva.

Dimensioni dei campioni [µm]	***MIT [˚C]***
1000-500	740
< 500	660
< 250	490
< 75	590

Le temperature minime di accensione (MIT) della polvere di sansa di oliva registrano un incremento da 590 ° C fino a 740 ° C inversamente proporzionale alla dimensione delle

particelle analizzate (del taglio granulometrico) in questo studio. Questo comportamento è noto nella letteratura scientifica sull'esplosione di polveri ed è determinato dal fatto che particelle organiche più piccole richiedano una minore quantità di energia per la devolatilizzazione rispetto a quelle più grandi in funzione della superficie specifica (Eckhoff R. , 2003). Infatti risulta disponibile una superficie maggiore per il trasferimento del calore e la propagazione della fiamma. Tuttavia, è anche possibile notare che le frazioni <250µm hanno la più bassa temperatura minima di accensione. Ciò non concorda con la tendenza osservata (figura 3) nelle altre frazioni del campione (<75, <500 e 1000-500µm). Questo potrebbe essere attribuito alla natura chimica delle frazioni di polvere di sansa di oliva. Come spiegato nella sezione 2.4, la sansa di oliva è un sottoprodotto del processo di estrazione dell'olio d'oliva, quindi è composta principalmente da polpa e noccioli rimaste in proporzione che possono variare a seconda del processo e della natura dell'oliva.

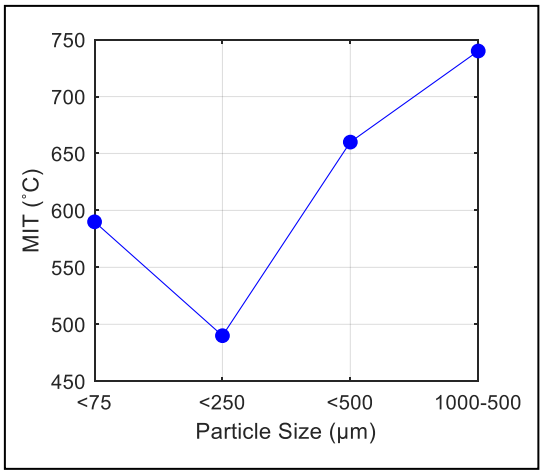

Figura 3: Temperatura minima di accensione delle frazioni <75, <250, 500-250 e 1000-500µm della polvere di sansa di oliva.

6 Temperatura di accensione di uno strato di polvere (LIT)

La tabella 9 riporta i dati acquisiti nella determinazione della temperatura minima di accensione di uno strato di polvere di 5 mm di campione di sansa di oliva con dimensione delle particelle <250 µm. Inoltre, in Fig. 4 sono mostrati i diagrammi termocinetici ottenuti durante le prove a temperatura rispettivamente pari a 280 e 290 ° C.

Tabella 9: Risultati dei test nel dispositivo su piastra riscaldante per polveri di sansa di oliva <250µm. N = nessuna accensione, P = accensione, x # indica il numero di accensione o nessuna accensione osservata.

Temperatura [˚C]	***Osservazione***
250	N
300	P
290	P
280	N x2

Secondo i dati presentati nella tabella 9, la temperatura minima di accensione dello strato di polvere della sansa di oliva con dimensione delle particelle <250µm è 290 °C.

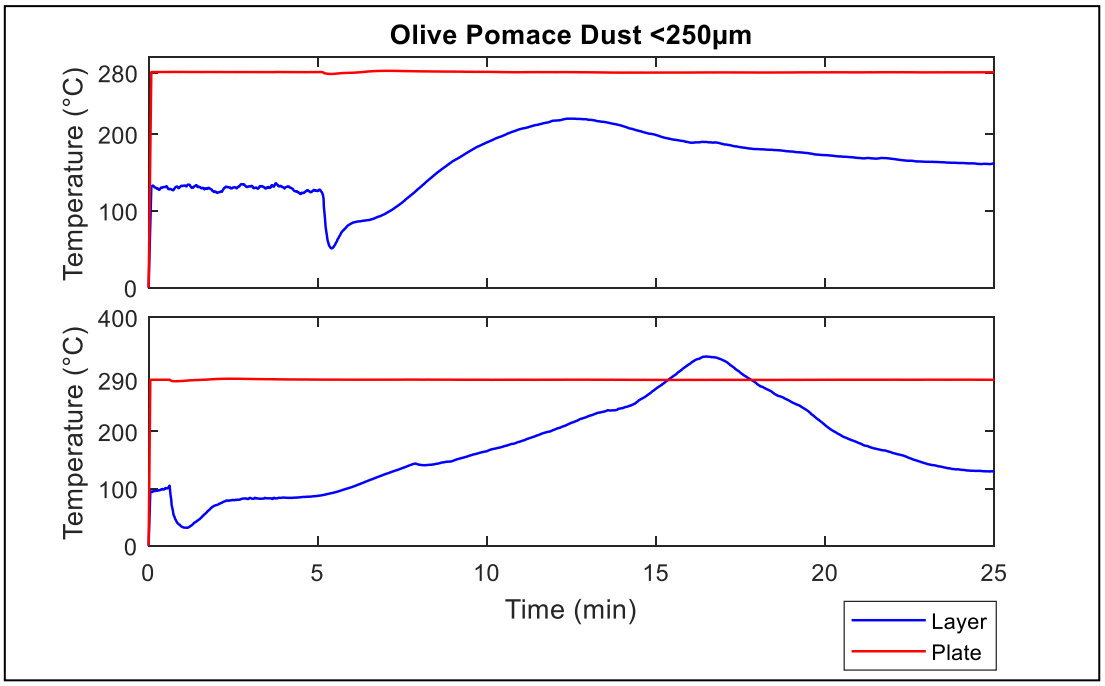

Figura 4: Diagrammi termocinetici della polvere di sansa di oliva <250µm, temperatura della piastra: a) 280 ° C e b) 290 ° C.

Inizialmente, la temperatura diminuisce perché il campione di polvere è stato aggiunto a temperatura ambiente sulla piastra con la temperatura impostata. Successivamente, la temperatura inizia ad aumentare, in questo periodo si verifica l'evaporazione dell'acqua e la volatilizzazione di altre sostanze presenti nel campione di sansa di oliva. La curva raggiunge un massimo, che è maggiore della temperatura della piastra nel caso della curva LIT a 290 °C, come risultato del calore generato dopo l'accensione. Infine, la temperatura dello strato di polvere diminuisce e si stabilizza, poiché non c'è più materiale disponibile per la combustione e l'aria penetra attraverso il materiale bruciato, raffreddandolo.

7 Parametri di esplosione- 20 l sfera

I campioni di polvere con dimensioni comprese tra 500 µm e meno di 250 µm sono stati sottoposti a test di esplosione nella sfera da 20 l, al fine di quantificare il parametro deflagrante Kst, la Pmax e il LEL.

L'evoluzione di (dP / dt) e di Pm in funzione delle concentrazioni per ciascuna serie di misure effettuate sono illustrate nelle figure 5 e 6. I dati di esplosività ottenuti sono riportati nella tabella10.

Tabella 10: Parametri di esplosività per i campioni di polvere di sansa di oliva.

Campioni [µm]	K_{St} *[bar m/s]*	P_{max} *[bar]*	$(dP/dt)_{max}$ *[bar/s]*	*LEL [g/ m³]*	*St class*
500-250	21.4	5.9	78.8	> 1250	1
< 250	49.4	6.8	182.1	200	1

È stato determinato che la polvere di sansa di oliva appartiene alla classe St1 (debole esplosione). Il valore Kst ottenuto per il campione con dimensioni inferiori a 250 µm è conforme a quello presentato nel database online dell'Istituto per la sicurezza e la salute sul lavoro della banca dati tedesca sull'assicurazione contro gli infortuni (IFA), per il pellet di olive.

D'altra parte, come previsto, per il campione con dimensioni comprese tra 500-250 µm, sono stati ottenuti valori K_{St} e P_{max} più bassi. Le particelle con dimensioni più ridotte portano a

esplosioni più violente, poiché queste particelle hanno una grande area superficiale che aumenta il tasso di combustione e la volatilizzazione.

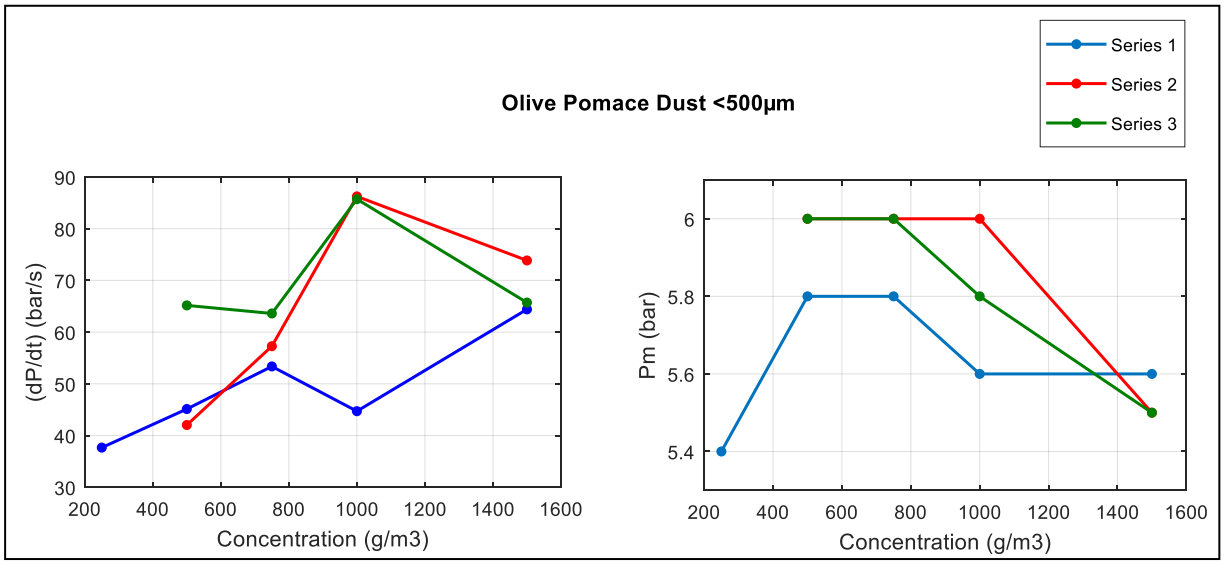

Figura 5: Valori della serie per la dimensione della polvere di sansa di oliva <250µm della velocità di aumento della pressione e dell'esplosione e della pressione in funzione della concentrazione di polvere.

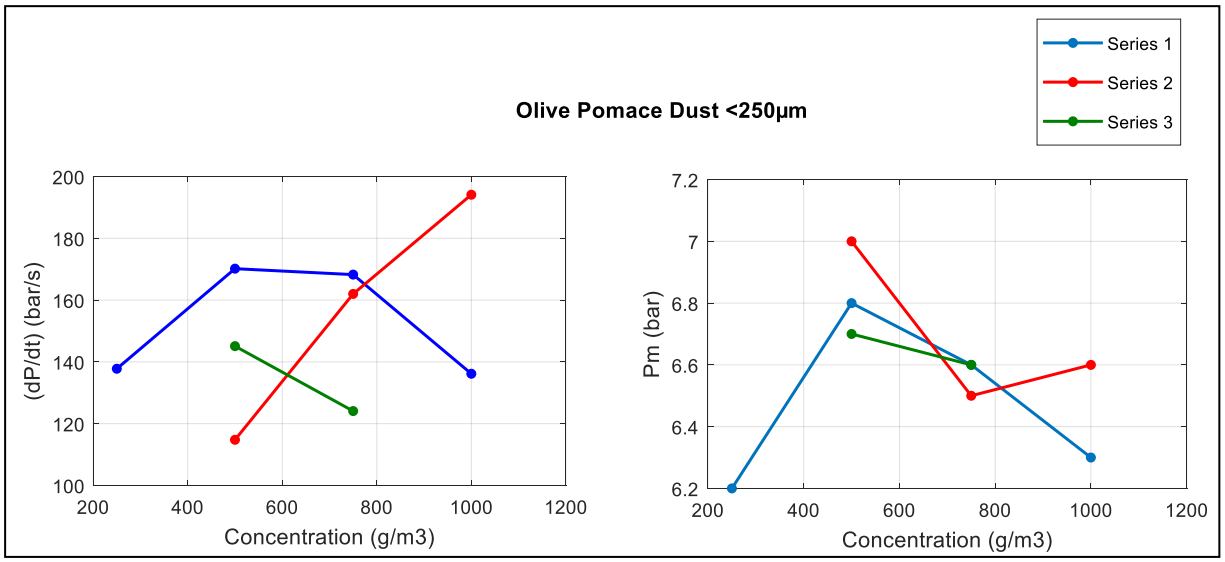

Figura 6: Valori della serie per la dimensione della polvere di sansa di oliva <500µm della velocità di aumento della pressione e dell'esplosione e della pressione in funzione della concentrazione di polvere.

Nella figura 7 e 8 sono rappresentati i valori della massima sovrappressione di esplosione Pm e la velocità massima di aumento della pressione di esplosione (dP / dt) massima ottenuta nella determinazione del LEL.

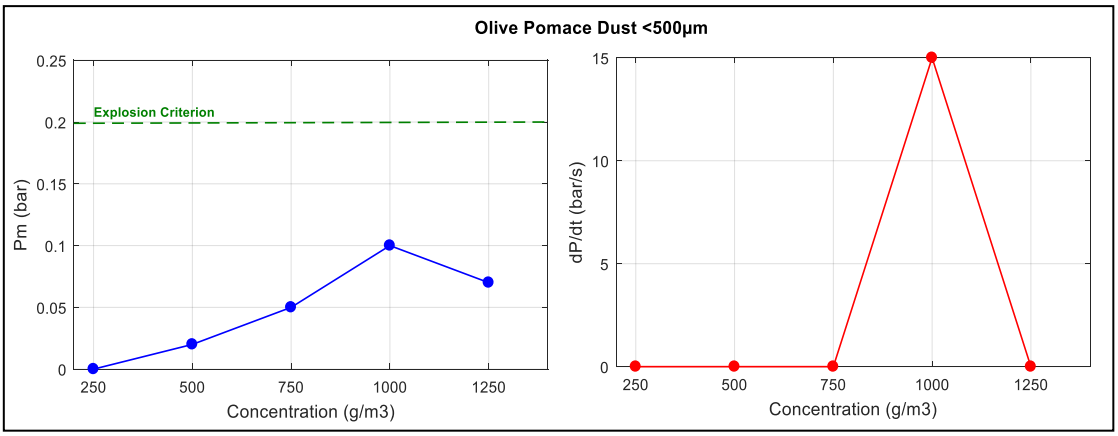

Figura 7: Variazione di Pmax e (dP / dt) con concentrazioni nella misurazione LEL per particelle di polvere di oliva con una dimensione <500µm.

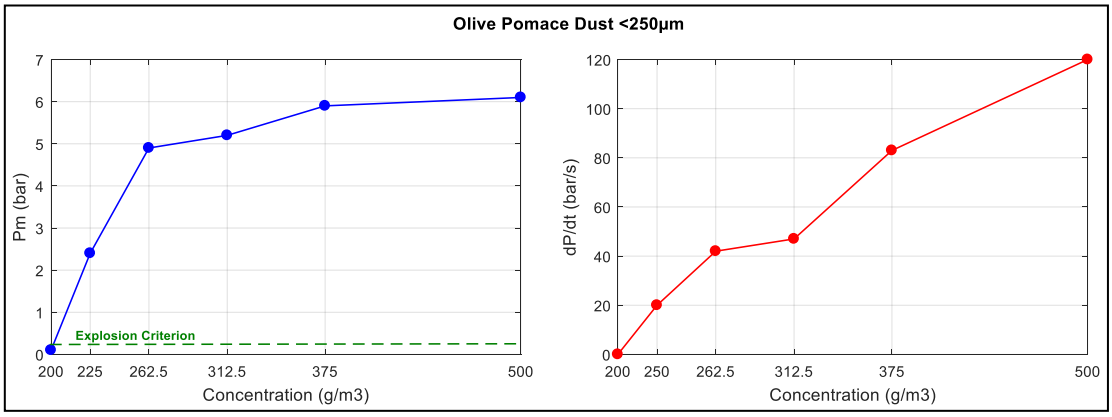

Figura 8: Variazione di Pmax e (dP / dt) con concentrazioni nella misurazione LEL per particelle di polvere di oliva con una dimensione <250µm.

I risultati dei limiti di esplosività inferiori (LEL) indicano che non si verificano esplosioni fino a concentrazione di polvere di sansa superiore a 1250g / m3 per particelle con dimensioni tra 500 e 250µm (una maggiore concentrazione non è stata testata, poiché potrebbero verificarsi problemi di intasamento all'imbocco della valvola con eccessive quantità di polvere), mentre per particelle inferiori a 250 µm, il LEL pari a 200 g/m^3.

8 Influenza del contenuto di umidità

Per amplificare la caratterizzazione esplosiva della sansa di oliva, Pietraccini M. (2019) ha determinato ugualmente i parametri deflagrante partendo dallo stesso campione di base (la temperatura minima di accensione (MIT) utilizzando un forno BAM, il limite inferiore di esplosività (LEL) e i parametri dell'esplosivo (P_{max}, (dP / dt) max e K_{St}). Tuttavia, Il campione è stato macinato in un mulino a martelli per ottenere le diverse frazioni da testare (legegrmente differenti dal lavoro presentato qin questa tesi); inoltre si è provveduto preliminarmente ai test ad essiccare il campione (in un forno ad aria a 110 °C per 24 ore).

Confrontando i risultati ottenuti in entrambi gli studi, è possibile affermare che quando il contenuto di umidità è inferiore, i parametri di esplosione P_{max}, dP / dt max e K_{St} aumentano. D'altra parte, la temperatura minima di accensione delle diverse frazioni diminuisce.

Nel lavoro di Pietraccini (2019) è necessaria una minore concentrazione di polvere di sansa per innescare l'esplosione (LEL) rispetto alla polvere utilizzata in questo test (dove il contenuto di umidità residuo è compresso fra 6,39% e 6,89%). Questo può essere spiegato

considerando che il riscaldamento e l'evaporazione dell'acqua agiscono come un dissipatore di calore/consumatore, attenuando il carattere esplosivo del campione. È importante tenere presente che le differenze tra i valori LEL dei due lavori è anche funzione della procedura seguita nelle misure. Pietraccini (2019) ha testato le polveri seguendo lo standard americano ASTM E1515-07 invece della EN 14034-3 (2006). Questo standard prevede l'utilizzo di un singolo accenditore chimico di energia pari a 2.5kJ. Mentre la normativa europea (usata in questo lavoro) stabilisce che per la misurazione del LEL dovrebbero essere usati due accenditori chimici da 1kJ, quindi l'energia di accensione totale utilizzata nel test pari a 2 kJ. Inoltre, la disposizione degli accenditori chimici all'interno della sfera nello standard americano è diversa da quella stabilita nello standard europeo (l'accenditore singolo è rivolto vs il basso, mentere si dispone la copia di accenditori da 1 kJ in modo che risultino perpednicolari rispetto all'ugello di dispersione della polvere).

Conclusioni

L'esplosività della polvere di sansa d'oliva risultante dall'estrazione dell'olio d'oliva è stata studiata in questo lavoro. Questo sottoprodotto è costituito principalmente da frammenti di nocciole e polpa delle olive lavorate, con valori di calore di combustione tra 4500-4600 kcal/kg.

Dal presente lavoro si possono estrarre le seguienti conclusioni:

• Il processo di macinazione della sansa di oliva ha un'influenza notevole sulla morfologia e sulla distribuzione delle dimensioni delle particelle.

• I risultati del test di screening hanno permesso di classificare la polvere di sansa di oliva come una polvere "esplosiva a temperature elevate".

• La dimensione delle particelle aumenta la temperatura minima di accensione di una nube di polvere. Tuttavia, la natura chimica della polvere di sansa d'oliva influenza questi valori di temperatura. Le diversi frazioni granulometriche hanno MIT compressa tra 490 °C e 740 °C.

• La temperatura minima di accensione di uno strato di polvere di sansa di oliva con dimensione delle particelle <250µm è pari a 290 °C.

• I risultati delle prove eseguite nella sfera di 20l classificano la polvere di sansa di oliva come appartenente alla classe ST1 (K_{St} pari a 21,4 e 49,4 bar m / s rispettivamente per le frazioni 500<d<250 e <250µm. Il K_{St} e la massima pressione di esplosione aumentano con la diminuzione delle dimensioni delle particelle.

• Il limite inferiore di esplosività LEL diminuisce con la riduzione della dimensione delle particelle. Le particelle con una dimensione compresa tra 500-250 µm non si sono innescate per valori di concentrazioni fino a 1250 g/m^3, mentre le particelle al di sotto di 250µm esibiscono un LEL pari a 200 g/m^3.

• Il contenuto di umidità ha anche un'influenza sui parametri deflagranti. Le polveri di sansa di oliva con un contenuto di umidità significativo hanno una temperatura di accensione minima più elevata e un limite di esplosività inferiore più alto. Il contenuto di umidità riduce i parametri esplosivi P_{max} e K_{St}.

Table of Contents

List of figures

List of tables

Nomenclature

Abbreviations

ASTM American Society for Testing and Materials

CEI Italian Electrotechnical Committee

EN International Standard

GG Godbert-Greenwald furnace

IFA Institute for Occupational Safety and Health of the German Social Accident Insurance

ISO International Organization for Standardization

LEL Lower Explosibility Limit

LIT Minimum Ignition Temperature of a dust layer

MIT Minimum Ignition Temperature of a dust cloud

OMW Olive Mill Wastewater

PSD Particle Size Distribution

SEM Scanning Electron Microscopy

Symbols

C Concentration	g/m^3
(dP/dt) Rate of explosion pressure rise	$bar \cdot s^{-1}$
$(dP/dt)_{max}$ Maximum rate of explosion pressure rise	$bar \cdot s^{-1}$
K_{St} Deflagration Index	$bar \cdot m \cdot s^{-1}$
P Pressure	bar
P_{max} Maximum explosion pressure	bar
P_{ex} Explosion pressure	bar
t Time	s
T Absolute temperature	℃
V Volume	m^3

1 Introduction

Dust explosion hazard represents a constant threat in the industrial processes that involve materials in the form of powders. These explosions can occur when very fine combustible particles are dispersed in a confined space with a source of ignition present. To avoid and prevent dust explosion in workplaces different laboratory tests was deigned to. Determine and characterize the tendency of the dusts to ignite, as well as the severity of the explosions that they can generate.

It is well known that in recent years the production of olive oil has increased in Mediterranean countries such as Spain, Italy, Greece and Turkey. However, the extraction of olive oil produces huge amounts of waste and by-products that have an environmental impact. These include the so-called "Olive wet pomace" (aqueous sludge) and olive pomace. The amounts of each depend on the nature of the olive fruit and the oil extraction technology applied. The two types of olive pomace contain pieces of pits, skin and pulp in different proportions. They differ in moisture content and chemical composition. Additionally, they are derived from different primary extraction technologies and are subjected to secondary extractions with solvents such as hexane.

Some works (Roig A. *et al.*, 2006; Abu-Qudais, 1996; Arif Hepbasli, 2003; Al-Ketan, 2012) studied the combustion of olive pomace and the potential that they have as an energy source in thermo-chemical conversion processes. Olive pomace is attractive as an alternative source of fuel. This is due to its high calorific value, its sulfur-free nature and the facility of obtain large amount from the extraction of olive oil processes.

From the processing of olive oil a product is obtained in the form of pellets, which can generate significant amounts of dust. Therefore, this work focused on determining the parameters, which characterize the deflagration of olive pomace dust. For this purpose, a physical characterization of a sample obtained from a two-phase centrifugal (decanter) olive extraction process was carried out, which consisted in the analysis of the particle size distribution, morphology, combustion heat and moisture content. On the other hand, the deflagration parameters: the minimum ignition temperature of a dust cloud (*MIT*), the minimum ignition temperature of a dust layer (*LIT*), the lower explosibility limit (*LEL*), the maximum pressure of explosion (P_{max}) and the deflagrating index (K_{St}) were measured in the laboratory facility Centro Sperimentale Sicurezza Industriale Atmosfere Esplosive of Politecnico di Torino. Additionally, a screening test was conducted prior to the test as to establish whether the powder sample was flammable or not, according to the ISO 80079-20-2:2016 standards.

2 Theoretical framework

2.1 Dust Explosion

Fine solid particles suspended in air can burn with a speed and violence that increases proportionally to the increasing subdivision of the particles (Eckhoff, 2016). For this reason, when a dust material is dispersed in a partially confined or confined space with an ignition source, an explosion can occur.

Additionally, it is important to consider that, in many cases, the dust explosion is a phenomenon that could propagate. Which means that a primary explosion could take place in a process unit and after might generate a second explosion in the process area. An initial explosion is originated by an amount of combustible dust in the presence of an ignition source, generating a blast wave that lift powder layers and create a suspended cloud. A secondary explosion initiates afterwards with the ignition of the dust dispersion by the flames of the primary explosion (Amyotte, 2013). The Figure 2.1 shows this meccanism.

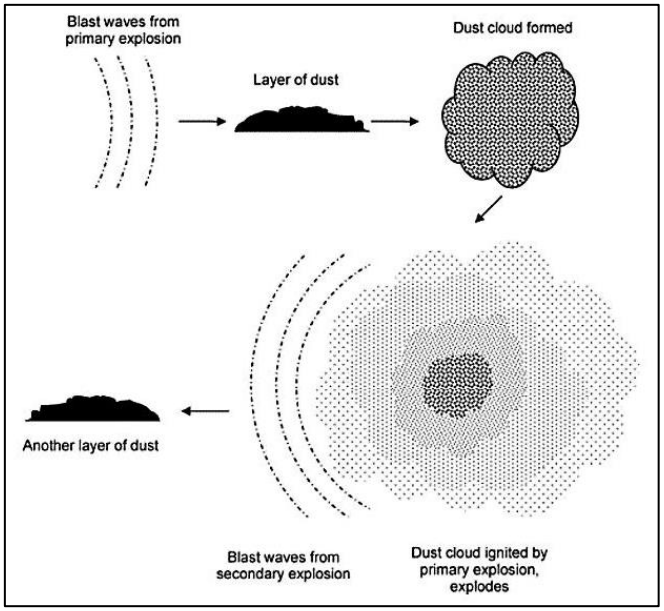

Figure 2.1: Primary and secondary dust explosion mechanism from Abbasi & Abbasi(2007)

2.1.1 Conditions for dust explosions

In order to understand a dust explosion causes, it is necessary append two more elements to the "*fire triangle"*, resulting in *"dust explosion pentagon"* (Kauffman, 1982) as illustrated in Figure 2.2. These elements are "confinement" and "dispersion". They have to be considered when the fuel, dust in this case, it is scattered in a limited area. The component "dispersion" of the pentagon, refers also to concentration. If the concentration is too low, there is not sufficient fuel to an explosion, otherwise, if it is too high, the quantity of oxygen to support combustion will not be enough (Ogle, 2016). Therefore, the necessary conditions are:

- Presence of combustible dust in a finely divided form
- Availability of oxidant
- Presence of an ignition source

- Partial or completely confinement of a dust cloud
- Dispersion of the dust particles

A dust explosion will occur when all factors of the pentagon are present and reach the explosive range (NFPA, 2007).

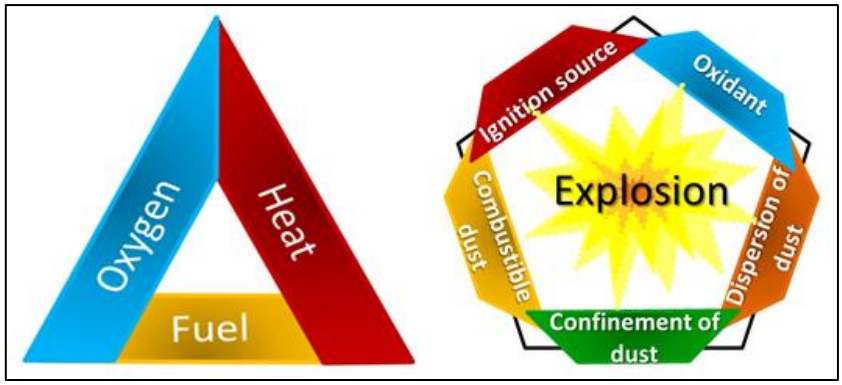

Figure 2.2: Fire Triangle and dust explosion pentagon

2.1.2 Factors influencing the flammability and violence of dust explosions

Some factors influence the ignitability and explosiveness of powders clouds. The most important of them are given below:

- *Chemical composition:*

  The chemical nature of dust influences thermodynamics and kinetics, it means, how much and how fast the heat is released of the reaction. In the determination of the total heat released in a dust explosion, it is the amount of heat of combustion by mole of oxygen. (Eckhoff, 2003). A powder with large heat of combustion by mole of oxidizer will emit a larger amount of thermal radiation, consequently, the maximum pressure and the intensity of explosion will be greater.

- *Particle size and surface area:*

  Broadly, the ignitability of a powder and the violence with it explodes increases when the particle size decreases. This is due to the finer particles have a greater surface area per unit of mass, also, those are more easily dispersed and remain suspended for longer periods (Abbasi & Abbasi, 2007).

  If the size of organic dust particles is very small, the devolatilization does not influences the explosion rate, in fact, further particle size reduction will not promote an increase in the combustion rate. Metallic powders instead, could have a smaller particle size and still influence the combustion rate, due to metal particles burn as discrete entities and do not yield a homogeneous combustible gas phase by devolatilization as organic materials do (Eckhoff R. K., 2009).

  Abbasi & Abbasi (2007) also explain the explosibility of dust does not vary linearly with the particle surface area, even though it depends on it. This reliance is dictated by the rate of combustion of volatiles and the concentrations of powders.

  It is also important to consider the degree of agglomeration. Small particles tend to form agglomerates (in mainly in the range below 10μm) (Eckhoff R., 2003), thereby the effective particle size becomes larger and the effective specific surface area decreases (Figure 2.3).

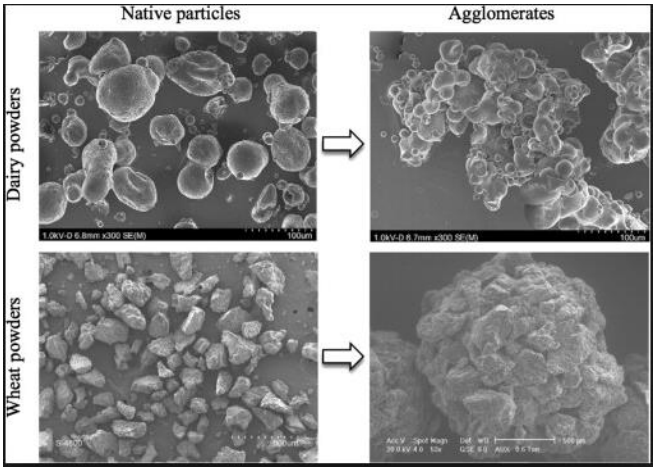

Figure 2.3: Scanning electron microscope picture of native particles and agglomerates of dairy powder and wheat powder, from Cuq et al. (2013)

- *Initial temperature and pressure of the dust cloud:*

  Chasdollar (2000) has showed the inversely proportional relationship between the initial temperature and the explosion pressure, as expected from the ideal gas law. This fact is due to that at higher temperatures there are less oxygen molecules for combustion. Therefore, for dust dispersion the explosion severity decreases with increasing of the initial temperature of the gas in the cloud.

  A rise of the initial pressure increases the initial turbulence in the dust dispersion, hence the explosion violence become greater. Additionally, Amyotte *et al.* (1990) found that there is a linear dependency between the P_{max} and the initial pressure.

- *Turbulence of the dust cloud:*

  The random movement of particles in the dust cloud in three-dimensional space generates turbulence (Eckhoff R., 2003). This degree of turbulence is responsible for maintain the powder dispersed in air. For high levels of turbulence, the flame front is broken up and its effective area is much greater, therefore the explosion will propagate faster and the explosion violence will be greater. For low levels of tubulence, the force of explosion can be relatively moderate (Barton, 2002). The level of turbulence reached is dictated by the geometric space where the explosion occur and the expansion induced flow of unburt dust cloud ahead of the propagating flame.

- *Dust concentration:*

A dust cloud may explode when the powder concentration is between certain limits. For higher concentrations when the mixture exceed the stoichiometric ratio, there is not enough exygen for complete combustion, thus the unreacted material will become a heat sink and the explosion force will be lower. The lower concentration limit is determined by the minimum quantity of fuel particles necessary to sustain the combustion (Abbasi and Abbasi, 2007)

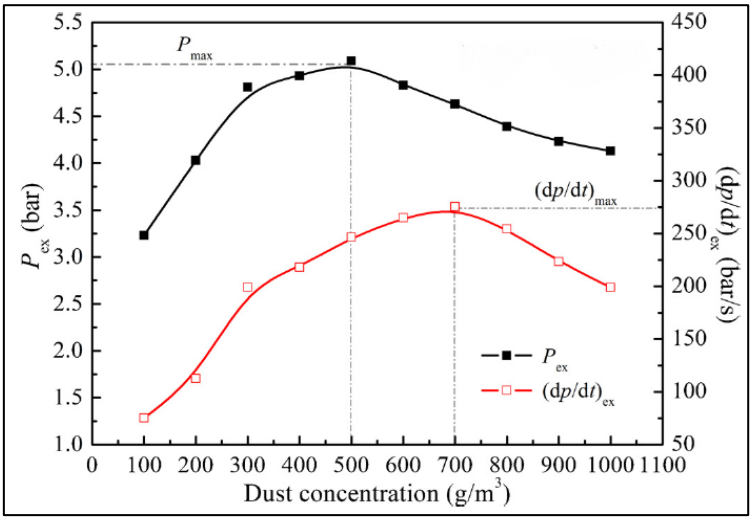

Figure 2.4: Variation of the maximum rate of explosion pressure rise (dP/dt) and the explosion pressure as a function of coal dust, from Jingjie Yuan (2014)

- *Radiative heat transfer:*

  Thermal radiation is an important heat transfer method in dust deflagrating and depends on the particle size distribution and dust concentration in the powder cloud. Dusts dispersions with high concentration of fine particles and large heat of combustion by mole of oxygen has a greater radiative heat transfer (Ogle, 2016).

- *Moisture content of the dust:*

The moisture in the powder affects the sensitivity to ignite and the violence of the dust explosion in different forms. Eckhoff (2003) explains that the pyrolysis gases in the preheating zone of the combustion wave mix with water vapor, consequently the gas mixture becomes less reactive. In addition, the heating and evaporation of water acts as heat sink. Jingjie *et al.* (2014) observed that due to there is a proportional relationship between heat consumption and moisture content, the intensity of explosion decreases slightly and as moisture degree increases (Figure 2.5). Another way is that moisture bring on the agglomeration of the particles, thus the degree of dispersion of the dust cloud decreases as the effective particle size increases.

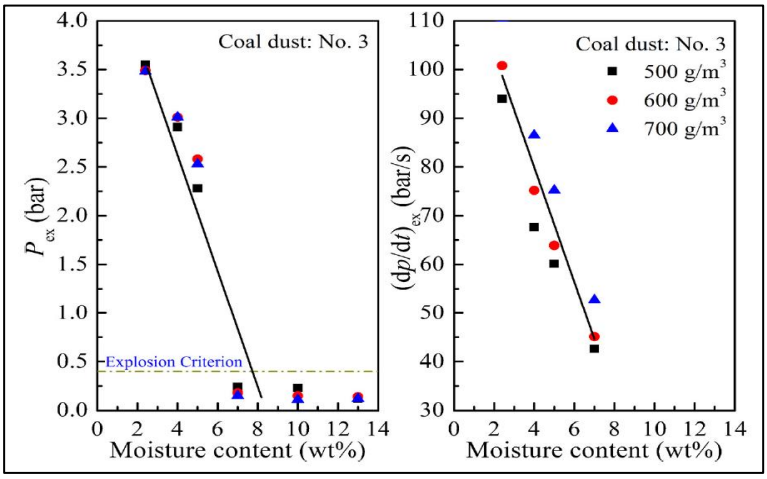

Figure 2.5: Influence of moisture content in coal dust on maximum explosion pressure and maximum rate of pressure rise in 20-L Siwek sphere, from Jingjie Yuan (2014)

2.2 Dust Deflagration Parameters

2.2.1 Minimum Ignition Temperature of a dust cloud (MIT)

The minimum ignition temperature of dust cloud is defined as the minimum temperature of the air for which a flame is generated because of the combustion of dust particles (A. Di Benedetto *et al.*, 2010). If a dispersion of dust if generated near to a hot surface whose temperature is approximately MIT, an explosion may occur. However, Eckhoff R. (Dust Explosions in the Process Industries , 2003) explains that the MIT depends on the geometry of the hot surface and the dynamic state of the cloud, consequently is not a constant value for a given dust cloud.

The MIT can be measured following the methodology established by ASTM E1491-06 (2019), using the 0.27-l Godbert-Greenwald furnace (explained in Chapter 3), the 0.35-l BAM Oven, the Bureau of Mines 6.8-L Furnace or Bureau of Mines 1.2-L Furnace. The unit of measurement is ˚C.

An industrial application of this parameter consists of limiting the working temperature of the equipment into which a dust cloud can be produced.

2.2.2 Minimum Ignition Temperature of a dust layer (LIT)

According to ASTM E2021−09 (2013) standard, the minimum ignition temperature of a dust layer is the lowest temperature at which a dust layer of specified thickness on a hot surface will self-heat.

In general, the minimum ignition temperature of a dust layer tends to decrease as the thickness of the dust layer increases (Lebecki, Z. Dyduch, & Sliz, 2003). This fact is due to the thermal insulation of the powder, which prevents the dissipation of heat towards the atmosphere. Therefore, the heat accumulated inside the layer, by heat conduction, produces a local temperature increasing with consequent self-ignition of the dust.

The LIT parameter is determined using a hot plate device and the unit used to measure it is ˚C.

2.2.3 Maximum rate of explosion pressure rise $(dP/dt)_{max}$

The normative EN 14034-2 (2006) defines $(dP/dt)_{max}$ as the maximum rate of pressure rise per unit of time during an explosion in a closed vessel; under certain test condition decreases with increasing the volume of the system. Moreover, the normative explains that this parameter could be determined by means of a differential calculation of the pressure-time curve obtained in experiments (see Figure 2.6). A common approach is the tangent method, which consists of extracting two points from the tangent line to the pressure-time curve at the inflection point. The following equation can be applied:

$$\left(\frac{dP}{dt}\right)_{ex} = \frac{P_2 - P_1}{t_2 - t_1} \qquad (P_2, t_2) > (P_1, t_1) \qquad [bar \cdot s^{-1}] \qquad (2.1)$$

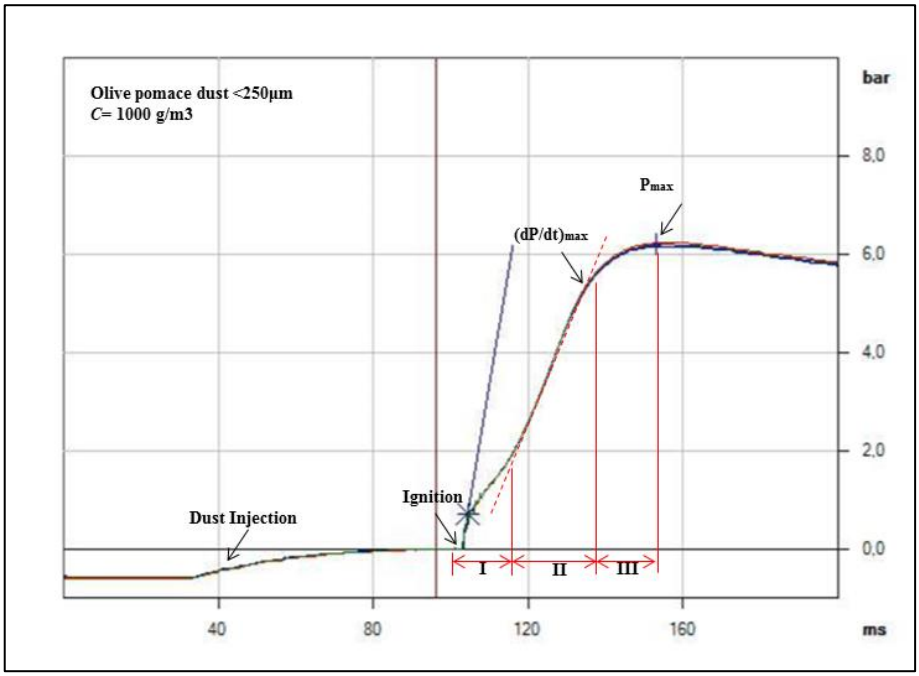

Figure 2.6: Typical p-t curve for olive pomace dust (C=1000 g/m3, particle size <250µm)

As can be seen in the figure 2.6, there are three stages during the dust propagation flame inside the 20l sphere (Kuai, *et al*., 2013):

- Period I: corresponds to the induction time t_i. During this time, the flame wave and the preheating of the particles before combustion are developed. As a result, there is a delay in the development of pressure.
- Period II: is denoted as t_{ii}. In this period the efficient propagation of the flame occurs as a consequence of the self-induced acceleration during t_i.
- Period III: its duration is defined as t_{ii}. In this period, the front of the flame has reached the wall of the chamber, while the rest continues to spread towards the walls.

The point of inflection between stages II and III corresponds to the moment in which the flame front encounters the walls of the vessel.

2.2.4 Deflagration index K_{St} and the "cube-root law"

The deflagrating index K_{St} [*bar m/s*] is an important parameter that characterizes an explosion severity. The contraction "*St"* comes from the German word "*staub"*, which meaning "*dust"*. This parameter also allows classifying the dust materials into four hazard classes as showed in table 2.1.

Table 2.1: Hazard classes for dust explosions, from (Cesana, G., & Siwek, 2016).

Range	Class	Explosibility
K_{St}=0	St_0	Non explosible
0 < K_{St} < 200	St_1	Weak
200 < K_{St} < 300	St_2	Strong
300 < K_{St}	St_3	Very strong

The Kst value is directly related to the maximum rate of pressure rise (dP/dt) by the "cubic root law" (equation 2.2). Bartknecht (1971, 1978) proposed this correlation.

$$K_{St} = \left(\frac{dP}{dt}\right)_{max} \cdot V^{1/3}. \quad (2.2)$$

where

$\left(\frac{dP}{dt}\right)_{max}$: *the maximum rate of pressure rise [bar / s]*

V: *the volume of the vessel*

K_{St}: *a constant for a dust [bar /m · s]*

2.2.5 Maximum explosion pressure Pmax

The maximum explosion pressure (P_{max}) is the maximum value of the overpressure relative to the pressure in the vessel (P_m) reached during an explosion at the time of ignition. It is determined by tests over a range of dust concentrations. The unit of measurement is *bar(g)*.

2.2.6 Lower explosibility limit (LEL)

Lunn G. (1988) provided a general definition of the lower explosibility limit (LEL) of an explosible substance (vapor, gas or dust), this is the lowest concentration of the fuel substance in air which will maintain a propagating flame.

This parameter may be obtained by the experiments in the 20 l sphere (section 3.6). The LEL is measured in g/m3. Additionally, can be used in the prevention of explosions in areas in which the explosive concentration of dust can be controlled.

2.3 Ignition Source

The dust explosions may not occur without the presence of an effective source of ignition with a sufficient amount of energy to initiate the propagation of the flame. Therefore, a fundamental preventive measure for explosions, consist of eliminate or avoid potential sources of ignition.

The main sources of ignition responsible to triggering the dust explosions are:

- *Self- heating*

  Echokff (2013), Abbasi & Abbasi (2007) explained that the self-heating on dust manifests as a slow combustion inside an accumulation of particles, it can occur as a consequence of exothermic reactions or situation in which there is a large amount of dust deposited in piles with a high initial temperature. This is aggravated by the porosity of the dust accumulations, which represents a fast access way for the oxygen to the surface of the particles, and at the same time decreases the thermal conductivity of the dust pile. Then, the heat generated in the initial oxidation may not be dissipated with a sufficient velocity to prevent an accumulation of it and a consequent increase in temperature. Hand in hand, as long as oxygen is still available, there will be an increase in the internal dust deposit temperature even further.

- *Friction and impact sparks*

  The rubbing between two bodies during a period can cause an increase in the dust temperature, or even worse, friction spark which can trigger an explosion in the presence of a dust cloud.

  The violent collision between two metal bodies can produce an impact spark, which would raise the temperature on the surface of one of them. The heat transferred from the surface to the inner part of the dust particles could represent a hazard.

  Some industrial processes use machines that operate with powder materials, which represent a dust explosion hazard if relevant preventive measures are not taken. An example of this is pulling the dust a drag conveyor (Abbasi and Abbasi, 2007).

- *Hot surfaces*

  J. Gummer and G. A. Lunn (2003) explain that a layer of dust in an accumulation could behave as a barrier to the dissipation of heat to the atmosphere. This is due to powders in general are not good conductors of heat. Therefore, the temperature of the rest of the dust can rise to the ignition point. In addition, they argue that depending on the nature of the dust, some of them may release flammable gases; while others may burn in the solid phase or melt and burn as liquids.

  A hot surface can ignite an accumulation of dust if it has a temperature compressed in the range of 100-200 ˚C. As referred in the Drier Guide of the IChemeE (Reay, 1977), which established as a preventive measure for hot surfaces that can serve as a source of ignition in dryers, that the entry temperatures must be at least 50 C below the minimum ignition temperature of the dust cloud.

- *Electrostatic sparks*

  For the ignition of dust dispersion through an electric spark, a minimum amount of energy is necessary, which depends on factors such as effective distribution of particle size, dust concentration and turbulence in a dust cloud, as well as the distribution of the energy during electric discharge, there will be a minimum energy of the spark.

(Eckhoff R. , 2003). The discharges originated by the release of electrostatic charge and glow or arcs formed at the moment when electrical circuits are broke, are considered ignition sources. It is particularly dangerous if the ruptures in thhe electrical circuits are small, since a stable arc can be generated.

Nowadays, the EN 1127-1:2007 standard identify as possible ignition sources the following elements:

- Hot surfaces
- Flames and hot gases (including hot particles)
- Mechanically generated sparks
- Electrical apparatus
- Stray electric currents, cathodic corrosion protection
- Static electricity
- Lightning
- Radio frequency (RF) electromagnetic waves from 104 Hz to 3 x 1011 Hz
- Electromagnetic waves from 3 x 1011 Hz to 3 x 1015 Hz
- Ionizing radiation
- Ultrasonic
- Adiabatic compression and shock waves
- Exothermic reactions, including self-ignition of dusts

2.4 Olive Pomace

Olive Pomace is a by-product derived from the olive oil processing, which is constituted by pieces of pit and pulp of the olive fruit, additionally, it has a certain content of oil and moisture that vary according to the process from which it comes.

2.4.1 Production process

In the olive oil production industry, there are two types of processes, including discontinuous process (traditional pressing) and continuous centrifugation process, the last is subdivided into three-phases centrifugation and two-phases centrifugation. In the Table 2.2 are summarized the input and output descriptions of the continuous and discontinuous olive oil production in order to compare them.

- *Discontinuous process: traditional pressing*

  According to Petrakis (2006), the production process begins with the cleaning of the olives. Initially, a strong airflow from an extraction fan is used, whose purpose is to eliminate leaves, branches and any type of dirt. Afterwards, they are washed with cold water, which comes from recirculation after washing mixed in a certain proportion with fresh water.

  The next stage of the process is performed by the hydraulic presses. During this phase of the process, the cells of the olive are teared, releasing the drops of oil. However, not all the oil is released because it is impossible to lacerate all the cells. In addition, amphoteric pseudomembranous which keep the oil in emulsion state, surround the oil drops, preventing the extraction.

  The olive paste derived from the crushing is subject to the malaxation phase. At this stage, the oil / water emulsions formed in the previous phase break, causing coalescence between the oil droplets. For this, a malaxing tank made of stainless steel with horizontal and vertical rotors is used, in addition, an outer jacket with hot water between 45-50 ˚C is integrated. The dough is kneaded through blades that have different shapes, made of stainless steel, which rotate slowly (15-20 rpm). Malaxation is a key step in the balance between the quantity and quality of the extracted olive oil.

  As the traditional pressing is concerned, Petrakis (2006) also explained that the traditional pressing technology consists of extracting the oil under pressure using hydraulic presses, its operated during 45-60 min, with gradually increasing of pressure up to 400atm, this value remains constant for 10-12 min. Subsequently, an amount of water is added to remove the solid material retained. Therefore, at the end of the process a pomace with moisture content of approximately 28% is obtained. In Figure 2.7 a description of it is presented.

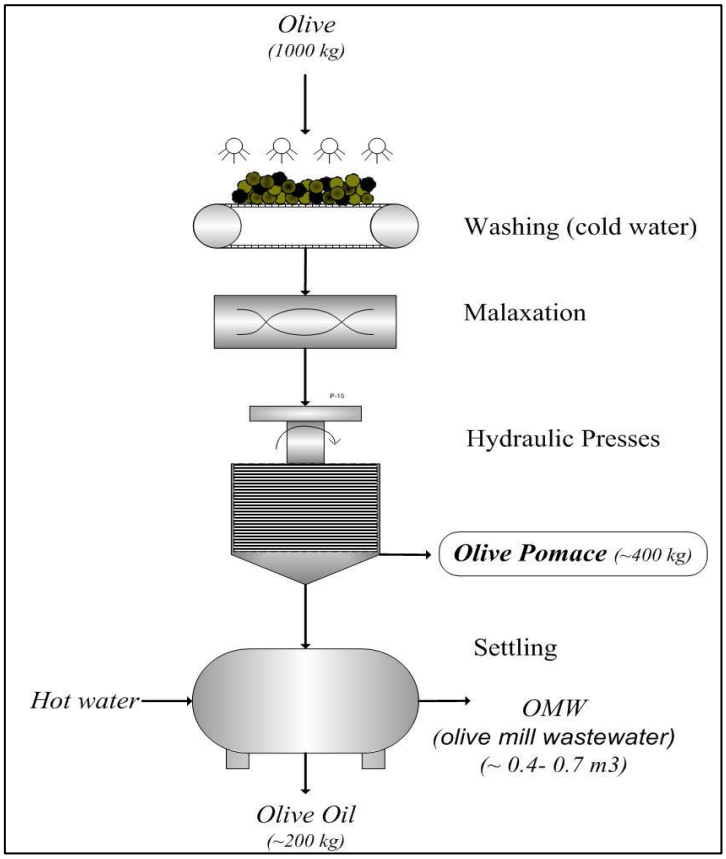

Figure 2.7: Traditional discontinuous pressing process.

➢ *Continuous centrifugation process*

The continuous process was developed as a solution to the need to produce olive oil in greater quantity and at a lower cost. With this objective, the hydraulic presses are replaced by a horizontal and two-phase centrifugal (decanter) system, which uses the centrifugal force to separate the liquid phase from the solid paste of olives. The initial part of the process is the same as the traditional method. The figure 2.8 shows the two types of continuous processes used for the olive oil production.

- *Three- phases centrifugation*

In the tree-phase centrifugation process, an amount of warm water is added, about 40-60% of the weight of the olives, in order to form a fluid paste that could facilitates the separation. Then, this diluted paste passes through a horizontal centrifuge. From this, three phases are obtained, consisting of an oily extract, vegetable water mixed with the added water (OMW) and pomace (45% moisture content). This process is more advantageous than the traditional one due to a higher quality of the oil. However, an important disadvantage is that since the water consumption is higher than the amount of waste water produced is about 1.25-1.75 times more compared to conventional technology (Petrakis, 2006). Additionally, this water in the initial wash removes a large portion of polyphenols. Therefore, it requires special treatment before being discarded.

- *Two- phases centrifugation*

On the other hand, the two-phases centrifugation process is similar to the tree-phases process, but differs in the amount of water used (lower in this case). It was created as an attempt to solve issues with the vegetation water waste treatment, because the amount of phenols in the water after washing is lower. A kind of sludge is obtained, also called

"Olive wet cake", it is constituted by pomace with 60-75% of moisture and certain quantity of sugars as a result of the water recycle (Arjona, Garcia, & Ollero, 1999).

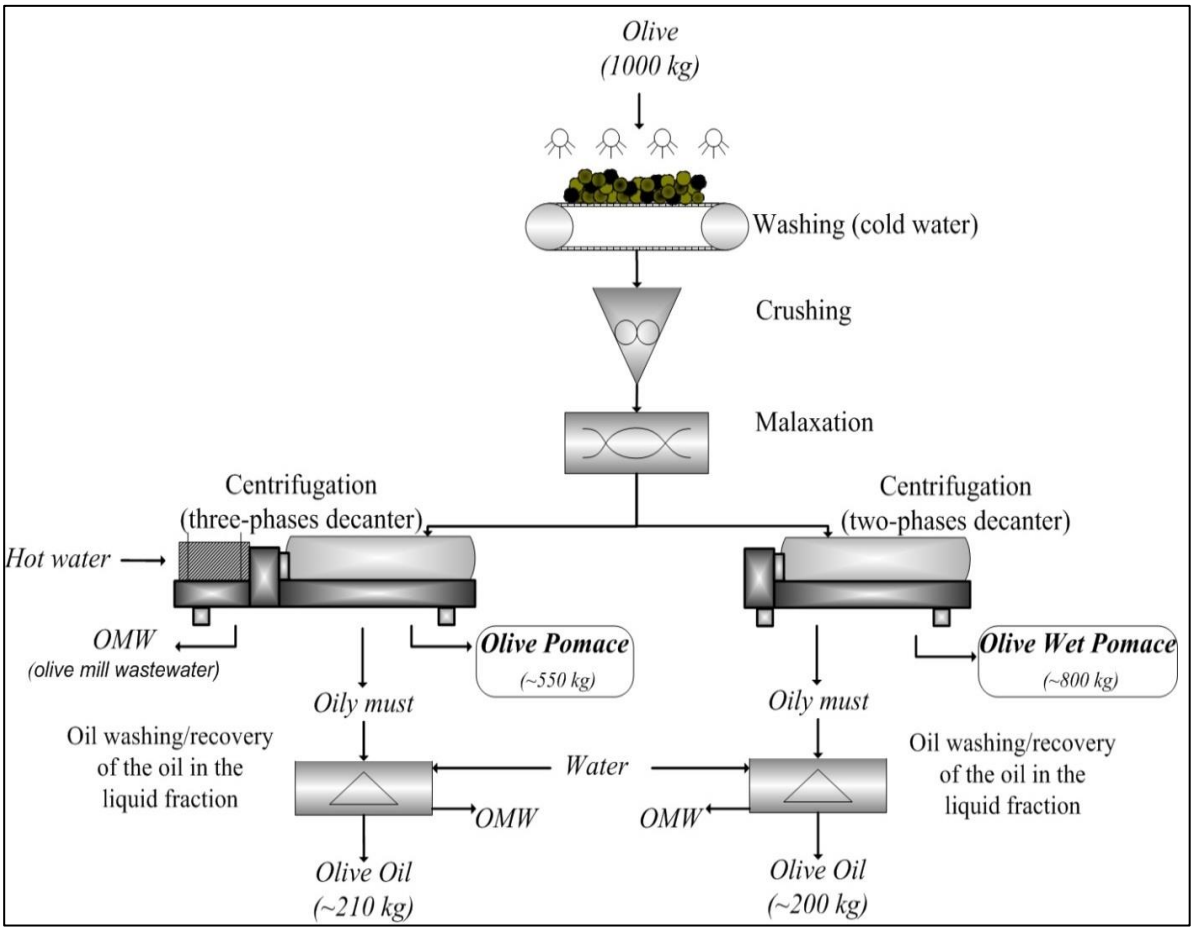

Figure 2.8: Continuous centrifugation processes.

Usually, the pomace obtained in the three different processes contains a certain amount of oil, which is economically convenient to recover. Whit this purpose, moisture content is reduced to at least 8% to obtain an efficient extraction (Mendez & Ruiz, 2006).

The reduction of moisture content in the olive pomace is done through a rotary dryer. This type of dryer is composed of a rotating cylinder supported on rolling strips. The speed of the rotation depends on the size of the cylinder, it can be simple or double step. In this process, drying gases at 400-800C are used, which can come, for example, from the burning of exhausted olive pomace derived after the recovery (Mendez & Ruiz, 2006).

Arjona R. (1999), explained that a high moisture contents (65% w/w) and a high amount of sugars present as consequent of the recirculation of the vegetable water, increase the tendency of the olive pomace to adhere to the walls of the drying cylinder. Specifically, at the entrance, hindering the flow of the hot gas stream and, consequently, increasing the risk of fire.

In the other hand, the chemical extraction phase is generally carried out in the following phases: first pulp is granulated, then the extraction with hexane is carried out and finally the desolventization of the pulp and distillation of the lean mixture is accomplished.

The final product is "*Olive exhausted Pomace*" and has a high combustion heat, which makes it attractive as biofuel.

Table 2.2: Comparison of the three types of olive oil processes (Anon, 2000)

	Input		***Output***	
Production process	***Description***	***Quantity***	***Description***	***Quantity [kg]***
Traditional pressing process	Olives	1000 kg	Oil	200
	Washing water	0.1–0.12 m^3	Solid waste 25% water 6% oil	400
	Energy	40–63 kWh	Waste water 88% water	600
Three-phase decanter	Olives	1000 kg	Oil	200
	Washing water	0.1–0.12 m^3	Solid waste 50% water 4% oil	500–600
	Fresh water for decanter	0.5–1 m^3	Waste water 94% water 1% oil	1,000–1,200
	Water to polish the impure oil	10 kg		
	Energy	90–117 kWh		
Two-phase decanter	Olives	1,000 kg	Oil	200
	Washing water	0.1–0.12 m^3	Solid waste 60% water 3% oil	800–950
	Energy	< 90–117 kWh		

2.4.2 Physical-chemical characterization

In the Table 2.3., are given some physical and chemical properties of the olive pomace derived from a second oil extraction process.

Table 2.3: Physical-chemical characteristics of olive pomace.Taken from G. Nicoletti (1999) with modifications.

Physical characteristics		
Physical state	Granular Solid	
Grain size	0.1- 4 mm	
Minimum Heat of combustion (dry residue)	4500 kcal/kg	
Effective volumetric mass density (Moisture 12-15%)	800-900 kg/mc	
Apparent volumetric mass density	500-700 kg/mc	
Volatile matter at 300 ° C	30%	
Volatile matter at 600 ° C	95%	
Ashes melting temperature	1150-1250 °C	
Chemical characteristics	min%	max%
Carbon	38.00	45.30
Hydrogen	4.00	5.50
Sulfur	0.01	0.04
Oxygen	20.00	34.00
Nitrogen	0.78	4.00
Moisture	7.00	23.00

The Institute for Occupational Safety and Health of the German Social Accident Insurance (IFA) provides the information about deflagrating parameters of only one olive pellets dust sample, reported in table 2.4.

Table 2.4: Explosibility parameters of the olive pellets dust.

Characteristics	
Particle size <63 μm [%by weight]	100
Median Value [μm]	<63
Lower Ex-Limit [g/m^3]	125
Max. Explosion Overpressure [bar]	10.0
K_{St} Value [bar m/s]	74
Explosibility	St 1
Minimum Ignition Energy [mJ]	>1000
Ignition Temperature BAM furnace [˚C]	470

2.4.3 Olive pomace as a source of renewable energy

The olive pomace is a by-product considered dangerous for the environment because it contains lignocellulose complexes. Specifically, olive wet pomace obtained in the two-phase process also contains soluble organic matter and fine solids, which are very dangerous to the environment due to their high demand for biochemical oxygen (BOD). The complex is considered non-biodegradable as only few enzymes can degrade the complex, and over long periods. Nevertheless, the presence of the lignocellulose complex facilitates the burning of olive pomace, thus favoring the production of energy (Al-Ketan, 2012).

The most common way to obtain energy from the olive pomace is through direct combustion. In fact, the direct combustion technology used is very similar to that used for coal. However, the complete combustion of olive pomace is easier to perform compared to the complete combustion of coal (Oktay, 2006).

A suitable combustion system for the olive pomace is a fluidized bed combustor as is showed in the figure 2.9 The fluid bed combustion system consists of a segmented steel cylindrical column. The upper part of the column has an air cooling jacket, which supplies preheated air to the fluidized bed. The olive pomace is fed to the bed from a hopper. Subsequently, the raw olive pomace moves downwards while the light ash rises and is removed in the upper part of the bed by means of a discharge pipe. Finally, the products of the combustion are sent to the cyclone connected immediately to the exit of the combustor in order to separate the solid particles from the gas stream. (Abu-Qudais, 1996). The efficiency of combustion depends on the size of the particles as well as the proportion of air / olive pomace fed.

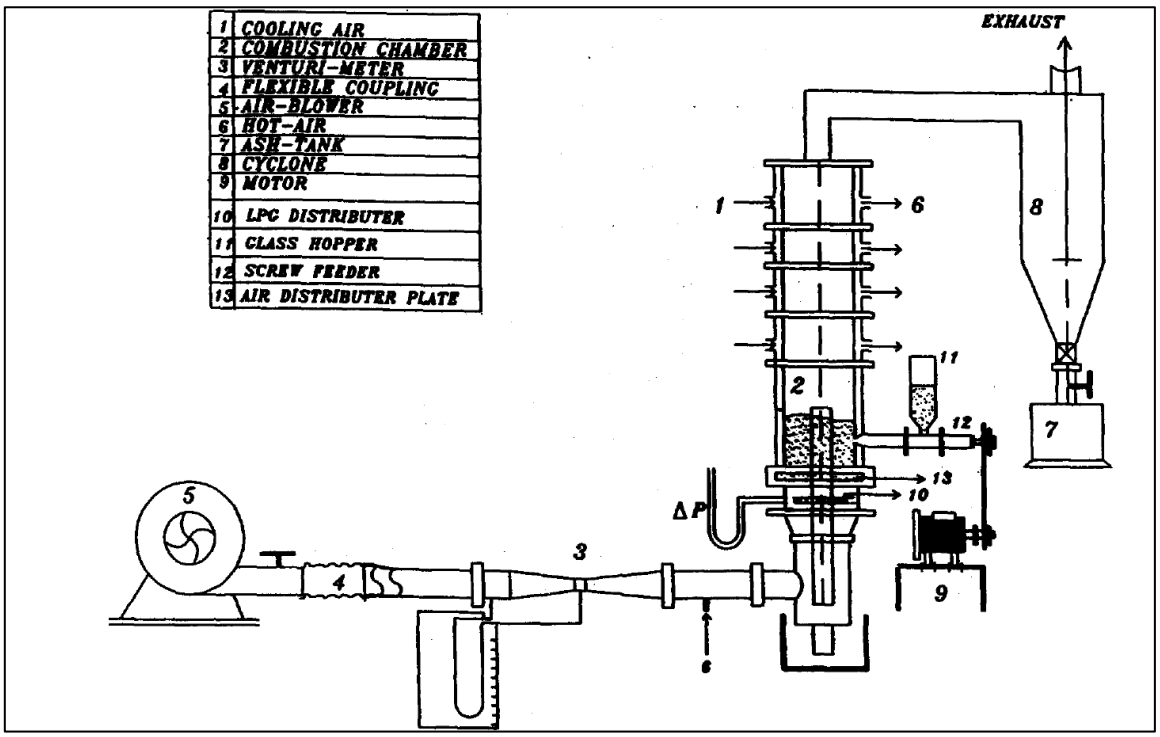

Figure 2.9: Scheme of fluidized bed combustor for olive pomace (Abu-Qudais, 1996)

Some studies (Arif Hepbasli *et al.*, 2003) (Alkhamis & Kablan, 1999) explain the potential of olive pomace as a source of renewable energy, and additionally, how its use would contribute to the reduction of polluting substances obtained in traditional coal combustion processes. Some of the advantages of olive pomace that make it attractive as a source of clean energy are its low sulfur content (almost negligible) and low cost (compared to many fossil fuels). The table 2.5 shows the percentages of emissions from combustion of olive pomace.

Table 2.5: Olive pomace combustion emissions, from Nicoletti (1999).

Temperature	490 ˚C
O_2	10.8 %
CO_2	10.4 %
CO	3700 (mg/Nmc)
NO_2	358 (mg/Nmc)
SO_2	< 0.5 (mg/Nmc)

3 Materials and experimental set up

3.1 Materials

The samples used in the different tests were obtained from a cutting pulverization of an olive pomace sample. This sample came from 2-phases centrifugation process and was therefore subjected to oil extraction (see fig.3.1).

From the pulverized material, the fractions between 1000 and 500µm, 500 and 250µm, <250µm and < 75µm were obtained for the analysis.

Figure 3.1: Olive pomace original and pulverized samples

3.2 Sample Characterization

3.2.1 Sieve analysis

As part of determining the particle size distribution (PSD), the sample was sieved. A vertical sieves assembly was used: 500 µm (ASTM nº 35), 250 µm (ASTM nº 60), 200 µm, 125 µm (ASTM nº 120), 75 µm (ASTM nº 200), 63 µm (ASTM nº 230) and 32 µm (ASTM nº 450). A sieve machine as shown in Figure 3.2, shook the sieves assembly for 10 minutes. Finally, the particle size distribution was obtained by weighing the remaining amount of dust on top of each sieve.

Figure 3.2: Sieve assembly

3.2.2 Laser diffraction

To obtain a more detailed granulometric distribution curve, a laser diffraction technique was applied using a laser granulometer (Malvern Mastersizer E100), according to ISO 13320:2009 standard. This technique is based on the diffraction of light, which consist of an expandable laser source that illuminates the particles presents in the measurement area, and the scattered light is measured with sensors on the focal plane of the lens. The scattered data is transformed into electrical signals, which are processed by the computer (Linchao Pan, 2017). The result is a granulometric curve with dimensions referred to 10, 50 and 90% by volume of the sample. The measurement range is 0.01-1000 µm. A scheme of the configuration of a laser diffractometer is illustrated in the Figure 3.3.

This technique does not distinguish between the morphology of the particles, that is, the dispersion of light cannot discriminate between electrical signals generated by spherical particles and those generated by other forms. Additionally, laser diffraction in opaque particles may result committed. Therefore, was convenient to apply this analysis and the sieve analysis to the sieved sample, in order to obtain results that are more accurate.

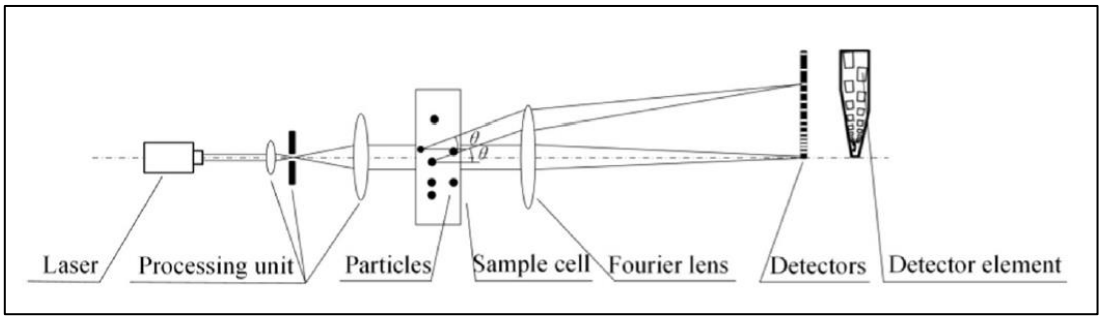

Figure 3.3: Configuration of a laser diffractometer (Linchao Pan, 2017)

3.2.3 Scanning Electron Microscopy (SEM) analysis

SEM technique uses the generation of a beam of primary electrons with high energy in the vacuums, focused through the lens and scanning a small area of the sample. The secondary electrons are emitted (backscattered X-ray electrons) by means of the interactions of the atoms that constitute the sample with the beam of the primary electrons. These electrons are part of the external atomic levels of the sample surface, which ones receiving enough energy from the incident beam and provide information about the morphology. The backscattered electrons,

there are those that are reflected and provide information of the sample composition level, given that their quantity depends on the average atomic number. In addition, X-rays are distinctive of the elements that make up the sample and can be differentiated according to length or energy. The secondary electrons are captured by a developer and subsequently converted into electrical impulses, which are then sent to a monitor in order to obtain an image with high resolution.

Dust sample was characterized using an electronic microscopy with a system of EDX FEI-Ispect S, column E-SEM W with a tungsten filament and an energy dispersive X-ray (EDX) probe. A magnification level of 500 X, 200X, 3.00 KX, 10.00 KX, 15.00 KX, 20.00 KX and 50.00 KX was applied.

3.2.4 Relative Humidity

The percentage of relative humidity was determined by weighing the dust mas. Subsequently, it was introduced in a laboratory stove at 65˚C for 5h. Finally, it was left to cool in a drying glass container with silica gel, which allows the cooling keeping the humidity constant in a short period. Then, the sample is weighed. To calculate the moisture value, the following equation was applied:

$$RH = \left(1 - \frac{Dry\ Weight}{Wet\ Weight}\right) \times 100 \tag{3.1}$$

3.2.5 Heat of combustion

The calorific power measurement was carried out in a constant volume calorimetric pump, according to ISO 1716:2018 standard. The sample is placed in a crucible inside an over: heat resulting from the combustion reaction of the fuel under examination is adsorbed by a known mass of water where temperature rise is checked. As the sample burns, the combustion gases heat the surrounding water. In this way, the temperature change in the water allows calculating the heat content of the fuel.

3.3 Dust combustibility testing (Screening test)

The screening test is constituted by four different tests, which are divided in two categories, the room temperature and the high temperature tests.

1. The room temperature tests are dived in:
    1.1 Dust ignition in the Hartmann tube- continuous arc
    1.2 Dust ignition in the Hartmann tube- glowing wire test
2. The high temperature tests are:
    2.1 Dust cloud autoignition in the GG furnace
    2.2 Dust layer autoignition in the hot plate

According to the dust behavior in the tests, it is possible to establish a classification. In case of ignition in any of the Hartmann tube tests, the dust is classified as "explosible at ambient temperature". If the dust sample is ignited during a high temperature tests, then the sample is classified as "explosible at high temperature". Otherwise, if the dust sample is no ignited in any test, is classified as "not explosible".

In case of no ignition in the 1.1 room temperature test, the test goes on to the next ignition source (more powerful, i.e. the coil wire). In the same way, if the dust do not ignite at ambient temperature it is necessary to execute the high temperature tests.

Subsequently, if the dust was defined as explosible, in order to characterize the explosion violence, the deflagrating parameters shall be determined.

3.3.1 Hartmann Tube- Continuous arc

The dust was submitted to screening tests at room temperature with continuous arc and glowing wire as sources of ignitions. The tests were performed on a Hartmann 1.2 L tube; it is made of glass with dimensions: 9 cm in diameter and 34.5 cm in height. The source of ignition is disposed inside the tube at the bottom.

The aim of the screening test with Hartmann tube is to analyze the sensitivity of the powder to an electrical ignition source with a certain quantity of energy when dust dispersion is formed at room temperature.

As established by EN 13821 (2004)standard, the ignition source in this test consists of an electric arc generated between two tungsten electrodes (see fig.3.4). They are placed perpendicular to the axis of the cylinder at a height of 11.5 cm from the bottom, separated by 6mm and connected to a control unit, which allows the passage of current, and consequently the formation of an electric arc of known quantity of energy (i.e. about W). The compressed air must have a temperature in the range from 20- 25 ˚C; besides, the pressure must be between 0.8-1.1 bar absolute.

Figure 3.4: schematization of Hartman tube

The dust samples were tested at different concentrations: mass sample of 0.3, 0.5 and 1g, which have nominal concentrations of 250, 420 and 833 g/m^3 respectively. They were uniformly distributed around the compressed air inlet. The tube is disposed vertically with the electrodes attached to the cables that provide the current passage. The top of the tube is closed with absorbent paper (it does not affect the pressure in the tube or the aero dispersion) in order to recreate a certain degree of confinement in the apparatus. The dust is aero dispersed through the blowing of compressed air at 8.0 bar into the base. After each attempt, it is necessary to clean the Hartman tube to avoid that dust residues alter the concentration of the cloud.

The spark energy used was 525mJ (10μF), this value refers to the lowest ignition sensitivity degree (EN 13821, 2004) and represents the worst possible conditions.

The normative provide that the air is injected and visual observation of the ignition is needed. The attempt shall be repeated 10 times for each concentration. Sparks not considered as an ignition.

In case a ignition is observed the test is ended and the sample is classified as "Explosive at ambient temperature". Otherwise, if no ignition is observed, the sample is subject to Hartmann tube with glowing wire test.

3.3.2 Hartmann Tube- Glowing wire

It has been observed that some dust clouds cannot be ignited with the continuous arc but in presence of an ignition source with greater energy as the growing wire, they ignite. Thereby, to determine if a dust sample dispersed in air presents a risk of explosion in the presence of an ignition source, this test follows the previous less energetic one.

The procedure is the same as with the continuous arc, the difference consist in the ignition surce an iron alloy (*Constantan*) wire replaces the electrodes. A continuous electric current of 13.1 A and 11.8 V is passed (i.e. a power output of about 150W), and it is enough to make the wire glowing and to reach a wire surface temperature of approximately 800˚C. The dimensions of the filament are 27 cm in length, 0.6 mm in diameter and is rolled up six spirals.

As the energy input is reached and the glow is crearly visible the air blow is injected.

The applied criteria that allows to classy: if a powder is explosive at room temperature or not is the same as that of the continuous arc test.

Figure 3.5: Hartmann tube with the wire

3.3.3 Dust cloud autoignition in the Godbert-Greenwald furnace

The Godbert-Greenwald furnace has a cylindrical geometry disposed vertically with an external diameter equal to 250 mm. The external structure is made of stainless steel. Inside, it has a tube open to the atmosphere in the bottom and it is covered with silica. The internal tube has 36 mm in diameter, surrounded by a metal resistance that heats it. Besides, the upper end is connected to the powder holder through a glass adapter. The furnace is designed to endure temperatures up to 1200˚C.

The dust is dispersed inside the furnace through a pulse of compressed air coming from a reservoir and then falls by gravity into the lower part. The details of the structure are presented in Figure 3.6.

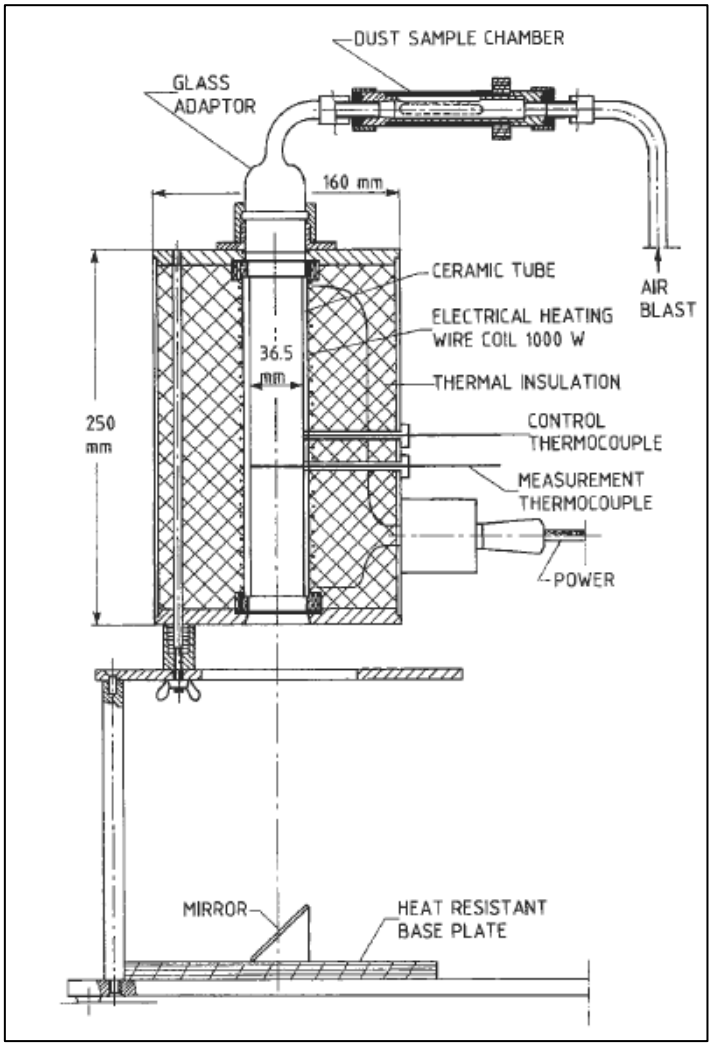

Figure 3.6: The Godbert-Greenwald furnace structure, from Eckhoff R. (2003)

The furnace is assembled on a metal plate that reflects the interior. In this way, it can be possible to appreciate the presence or not of an ignition

A pair of thermocouples is used to continuously measure the temperature. One of those is connected to the temperature controller for the furnace and the other to a digital thermometer that monitors the interior temperature. The PID controller regulates the current that passes through the internal resistance in order to maintain the temperature at set-point value.

This test allows verifying if the dust sample can be ignited or not when it is exposed to an ambient at high temperature. Specifically, the analysis was carried out at 800˚C, as established by the ISO 890079-20-2:2016.

Different concentrations of dust are tested in the oven, namely 0.1, 0.3 and 0.5 g of dust sample, applying an overpressure of about 0.3atm in the sample chamber. The test was performed until an ignition of the dust was observed or ten attempts without ignition before classifying the sample.

3.4 Minimum Ignition Temperature of a dust cloud

3.4.1 Test apparatus

The measurement of the minimum ignition temperature of a dust cloud (MIT) is determined with the Godbert-Greenwald furnace.

As for the screening test in the GG furnace, the dust sample was tested at different concentrations (0.1g, 0.3g and 0.5g), applying the same overpressure. The test was started with a temperature of 500˚C and it proceeds with an increase of 50˚C for each shooting until an ignition was observed. Once the dust dispersion was ignited, the temperature was decreased 20˚C until ten consecutive no-ignition tries. The Figure 3.7 shows the used furnace in the laboratory during the thesis work.

The normative CEI EN 50281-2-1 (1999) establishes that the Minimum Ignition Temperature would be the last temperature measured in the test (where an ignition occurred) reduced by 20˚C if it is greater than 300˚C and by 10˚C if it is smaller.

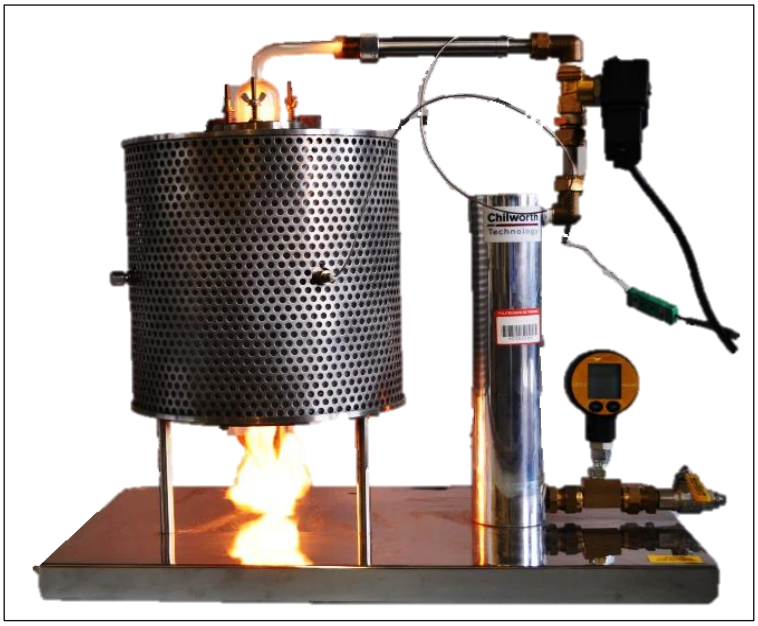

Figure 3.7: Godbert- Greenwald furnace

3.5 Hot-Surface Ignition Temperature of Dust Layers

The test consists of heating a layer of powder on a plate, following the procedure established by the CEI EN 50281-2-1 (1999) standard.

3.5.1 Hot plate device

The LIT was measured using a hot plate testing device from Chilworth Technologies, model 5 mm-LIT-H. It is made of an aluminum plate, over which the dust is placed inside a metal ring which defines the layer (sized 5mm in height and 100mm in diameter).

The temperature is monitored by thermocouples. One of them measures the temperature of the hot plate and is controlled by a PID controller, while the other one measures the temperature of the dust layer.

The plate was heated electrically up to a temperature of 250˚C. On the center of the heated surface, the metal ring was placed. Then, it was filled with the sample of the olive pomace dust, which particle size was <250µm.

Different criterion assesses the ignition of the sample:

- A temperature of 450˚C was measured
- A temperature greater than 250˚C respect to the temperature of the plate
- Visible glowing or smoldering in the layer

If in a period of 30min, no self-heating occurred, the test was stopped and repeated at a 50˚C above the plate temperature. However, in case of ignition, the test has to be repeated at a 10˚C below the previous temperature in which an ignition was observed.

The test was continued until it was found a temperature at which no ignition occurred in two attempts.

The final value of the LIT was the minimum temperature at which the ignition occurred decreased by 10 °C.

3.6 Tests in 20l Siwek Sphere

The dust sample was tested in a concentration range from 250 g/m^3 up to 1000 g/m^3. All the tests were performed in 20 l sphere, according to standards of table 3.1

Table 3.1: Procedures for measuring deflagrating parameters.

Deflagrating Parameter	***Standard***	***Igniters***
$\mathbf{P_{max}}$	UNI EN 14034-1: 2004+ A1:2011	2* 5 kJ
$\mathbf{K_{St}}$	UNI EN 14034-2: 2006+ A1:2011	2* 5 kJ
LEL	UNI EN 14034-3: 2006+ A1:2011	2* 1 kJ

3.6.1 Test apparatus

The explosion vessel is a sphere with a volume of 20 L, made of stainless steel. The sphere has a water jacket for cooling of the vessel after any explosion. The dust inlet in the explosion chamber is through a valve inlet in the bottom, in which compressed air is injected. The ignition source is positioned in the center of the sphere. In the upper part it is closed with a cover of the same material and has two supports for the chemical igniters. A pair of pressure transducers measure the explosion pressure wave and are connected to a control unit KSEP310. Figure 3.8 shows the structure and components of Siwek Sphere.

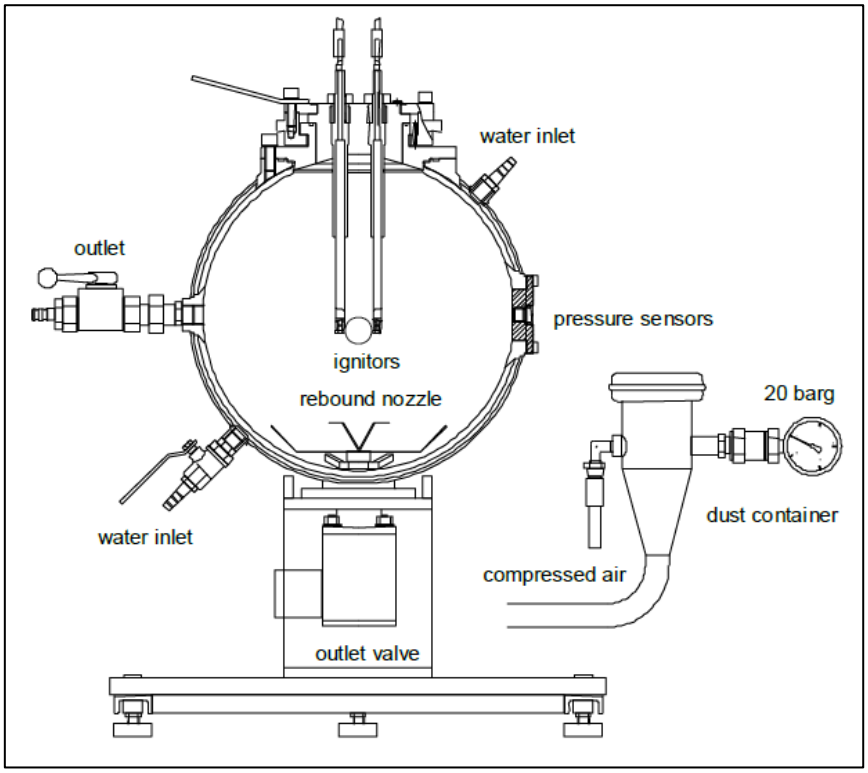

Figure 3.8: Vertical cross section of the 20 L Siwek Sphere (Cesana, G., et al., 2016)

The dispersion system consists of a dust chamber designed to tolerate an overpressure of 20 bar, a rebound nozzle and a fast acting pneumatic valve. Previously to dispersion, the explosion sphere was evacuated creating a depression level in the volume, in order to obtain atmospheric pressure inside it at the same moment of the injection of the dust sample. By opening a manual valve, it is possible to operate the vacuum pump to obtain the desired vacuum degree, which compensate the 20 bar overpressure of the inlet dust chamber.

The ignition source used consists of two chemical igniters with an amount of energy that varies according to the test performed, that is, from 1 kJ to 5 kJ. These igniters are used in pairs for each test. The chemical igniters shall be positioned in the center of the sphere, pointing in opposite directions. The figure 3.9 shows a picture of the inside of the 20l sphere at the instant when the chemical lighters are lit.

Electrical fuse heads are used to fire the chemical igniters. According to the normative (EN 14034-1, 2004+ A1 2011) the power circuit for the igniters must be able of firing the fuse heads in less than 10ms.

The activation and data recording system is composed by the control unit KSEP310, measuring and control unit KSEP332 and analysis software KSEP 7.0.

Figure 3.9: Photo of the chemical lighters lit inside the 20l sphere, from Skřínský, (2017).

The unit KSEP310 is linked to the entry of compressed air and the vacuum pump. Through KSEP332 system, the times of activation of the chemical igniters and the opening of the electro valve are controlled. Additionally, it receives signals from the piezoelectric pressure sensors that measure the pressure as a function of time, which are positioned on the internal wall of the sphere. Therefore, it is connected to the computer software. The KSEP 7.0 receives the signals, analyzes them and finally, provides results in terms of maximum explosion pressure and the pressure curve as a function of the different concentration tested. Due to the effects of pressure caused by detonation and the cooling of the inner walls, the software corrects the explosion pressure measured (P_{ex}) with the follow correlation:

$$P_m = 0{,}775 * {P_{ex}}^{1{,}15} \tag{3.2}$$

3.6.2 Test procedure

3.6.2.1 Maximum Pressure P_{max} and Deflagration Index K_{St}

To start the test, the chemical igniters were placed using the appropriated antistatic clothes.

The outer ends of the igniters holder were connected to the KSEP310 unit. Then, the amount of dust sample was introduced into the dust container.

The sphere was depressurized to -0.6 bar using the vacuum pump, while the dust container was pressurized to 20 bar using the compressor. Finally, the KSEP 7.0 was activated and, through an electrical signal, the quick action valve was opened. Due to the overpressure in the container, the sample was dispersed inside the sphere.

The ignition source consisted of two chemical igniters with an amount of energy equal to 5kJ each (10kJ in total).

The delay time between dust dispersion and activation of ignition source was 60ms (value established by the normative).

3.6.2.2 Lower explosibility limite (LEL)

The lower explosibility limit (LEL) was determined following the operative procedure stablished in the EN 14034-3 (2006). The test started using 10.00 g of dust sample, according to the normative, the test was repeated reducing the initial mass by 5.00 g until there is no evidence of an explosion. The energy of the ignition source for this test is 1kJ each (2kJ in total)

The KSEP manual (Cesana, G., *et al.*, 2016) establishes as explosion criteria the values reported in table 3.2.

Table 3.2: Explosion criteria adopted for determining LEL.

P_{ex} [bar]	P_m [bar]	Result
< 0.5	< 0.2	*No explosion*
≥ 0.5	≥ 0.2	*Explosion*

3.6.3 Calculation of $(dp/dt)_{max}$ and K_{St}

The methodology explained below was applied in accordance with EN 14034-2 (2006+ A1:2011) standard.

To estimate the rate of explosion pressure rise $(dp/dt)_{ex}$, the tangent method was applied, (see Chapter 2).

In total three series with different values of concentration were defined. The arithmetic mean of the maximum values of rate of explosion pressure rise for each series was determined to calculate the maximum rate of explosion pressure rise $(dp/dt)_{max}$, using the following equation:

$$\left(\frac{dP}{dt}\right)_{max} = \frac{\left(\frac{dP}{dt}\right)_{ex\,(series\,1)} + \left(\frac{dP}{dt}\right)_{ex\,(series\,2)} + \left(\frac{dP}{dt}\right)_{ex\,(series\,3)}}{3} \quad [bar \cdot s^{-1}] \tag{3.2}$$

The maximum explosion pressure was determined as the arithmetic mean of the maximum explosion pressure of each series (see equation 3.3).

$$P_{max} = \frac{P_{m\,(series\,1)} + P_{m\,(series\,2)} + P_{m\,(series\,3)}}{3} \quad [bar] \tag{3.3}$$

The K_{St} value was calculated with the equation 3.5 (valid for the 20 l sphere).

$$K_{St} = 0.271 \times \left(\frac{dP}{dt}\right)_{max} \quad [bar \cdot m \cdot s^{-1}] \tag{3.4}$$

3.6.4 Overdriving phenomena

The overdriving occurs when the ignition source is too strong in relation to the size of the test volume. The products of the combustion of the dust particles remain near to the flame adding energy and favoring the propagation, therefore the pressure increases. On the other hand, the energy released by the source of ignition preheats and burns the particles, affecting the pressure wave of the explosion.

An alternative to prevent the overdriving is accomplished the test on greater volume equipment, such as in the sphere of $1m^3$.

In order to discard a false positive in the previously obtained results, an attempt was made with 10 g of sample using two igniter of 1 kJ each. The effect of overdriving is ruled out if the explosion happens. The criterion that was adopted is based on the explosibility test procedure found in Siwek sphere manual (Cesana, G., *et al.,*2016), which defines an explosion to be occurred if an overpressure of 0.2 is registred.

4 Experimental results and discussion

4.1 Particle size distribution (PSD)

The particle size distribution (PSD) results obtained from sieving and laser diffraction are reported in table 4.1.

Table 4.1: PSD measured by sieving and laser diffractometry.

Sieve analysis		***Laser diffraction***					
Sample characterization		***Undersieve < 500 µm***		***Undersieve < 250 µm***		***Undersieve < 75 µm***	
PSD [µm]	***%w***	***PSD***	***µm***	***PSD***	***µm***	***PSD***	***µm***
< 32	1.03	**d(0.1)**	97.913	**d(0.1)**	31.816	**d(0.1)**	10.631
32-63	4.94	**d(0.5)**	354.954	**d(0.5)**	173.125	**d(0.5)**	36.246
63-75	5.61	**d(0.9)**	682.648	**d(0.9)**	351.656	**d(0.9)**	82.520
75-125	8.70						
125-200	18.05						
200-250	12.24						
>250	48.59						

According to the results presented in table No.4.1, a common factor is observed between sieving analysis and laser diffraction analysis, that is, the crushed sample of olive pomace was composed mainly of particles with dimensions greater than 250µm. Additionally, even though the samples analyzed in the diffractometer laser were previously passed through the 500, 250 and 75µm sieves, the instrument detected that 90% in volume of the particles had sizes greater than these. This inconsistency is due to the fact that the original sample of olive pomace was initially subjected to a crushing cuts process, from which some particles were formed with almost spherical shape and others more elongated (fiber-like). These elongated particles due to the vibrations in the sieving process could cross the sieve perpendicularly. In any case, it can give unreliable results for non-spherical particles

In the figures 4.1- 4.3 are presented the cumulative dust particle size distributions and the differential distribution of dust particle size, obtained for olive dust sample with size <500 µm, < 250 µm and <75 µm.

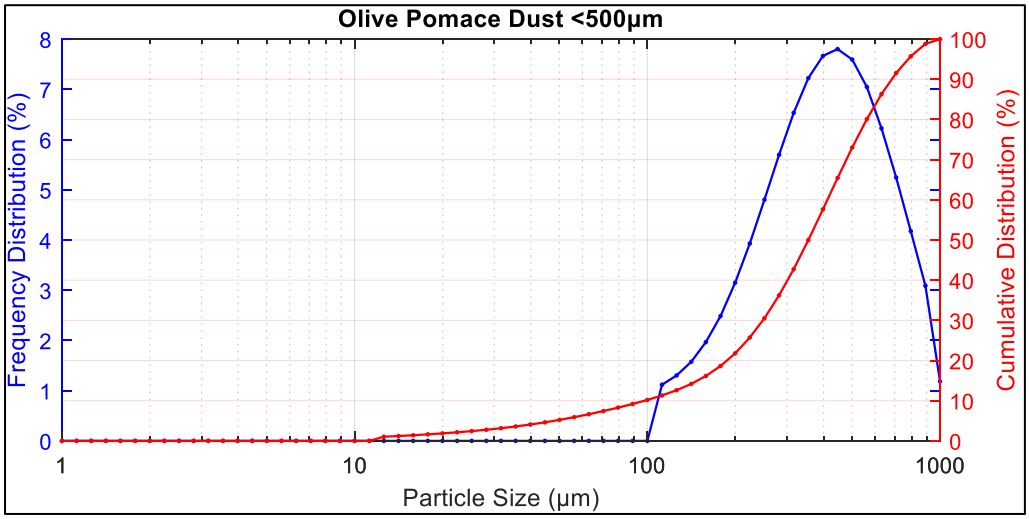

Figure 4.1: Cumulative and differential PSD of the olive pomace dust fraction <500µm

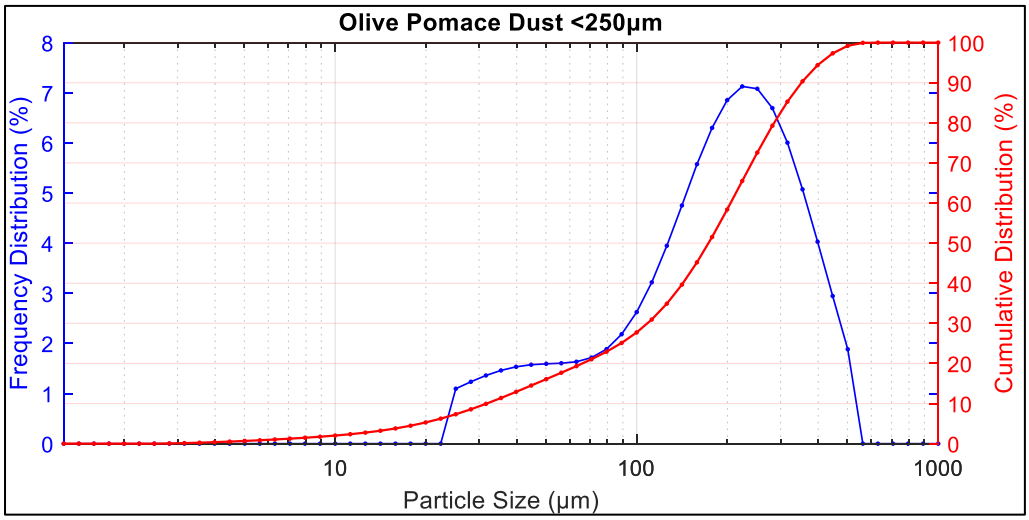

Figure 4.2: Cumulative and differential PSD of the olive pomace dust fraction <250µm

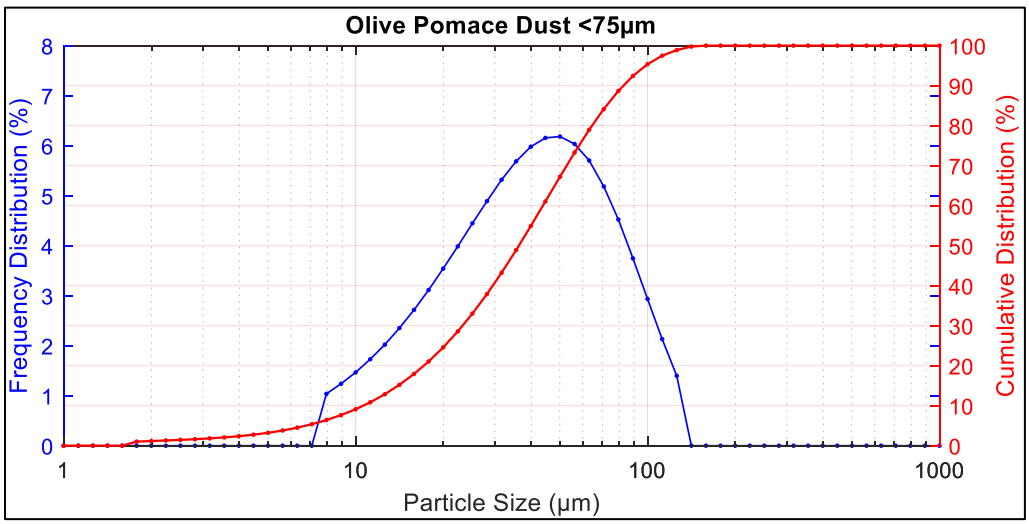

Figure 4.3: Cumulative and differential PSD of the olive pomace dust fraction <75µm

4.2 Analytical Data

The olive pomace dust was also characterized through the determination of moisture content and higher calorific value (HCV). The results are given in table 4.2. and 4.3..

Table 4.2: HCV of olive pomace dust sample.

Dust sample	*Higher heating value [kcal/kg]*
500-250 µm	4594
< 250 µm	4669

The difference between the values of heat of combustion determined is because the calorific power of olive pomace is influenced by pulp / stones ratio (Doymaz *et al.*, 2004).

The partition of pulp and stone was not considered in the present work.

Table 4.3: Moisture content of the olive pomace dust fractions.

Dust sample	*Moisture [%w]*
1000-500 µm	5.03
500-250 µm	6.39
< 250 µm	6.89
<75 µm	6.44

As expected, the moisture content and heats of combustion determined agree with those reported in section 2.4 for the olive pomace derived from a second oil extraction process.

4.3 SEM images

The morphological characterization was accomplished by images of the Scanning Electron Microscopy exhibited in Figs. 4.4 to 4.7.

It seems quite evident that the granular shape predominates in most of the particles (Figures 4.4 and 4.5), as well as the elongated forms, which resemble the structures of the wood chips (Figure 4.5). On the other hand, a magnification on the surface of the particles (see Figs 4.6 and 4.7) reveals the presence of channels within the particles. This suggests that olive pomace is a porous material with a relative high surface area.

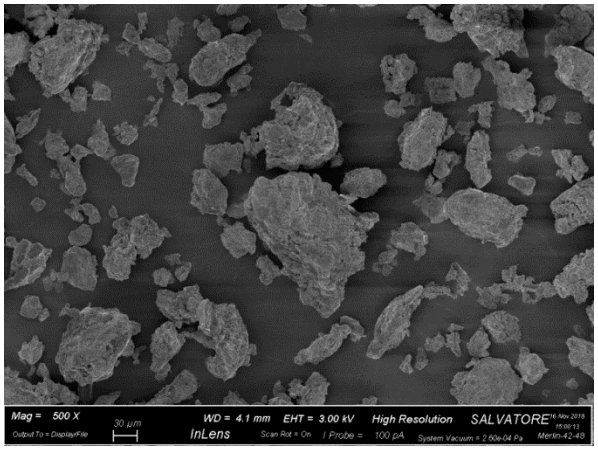

Figure 4.4: SEM image of olive pomace dust sample, 500x magnification.

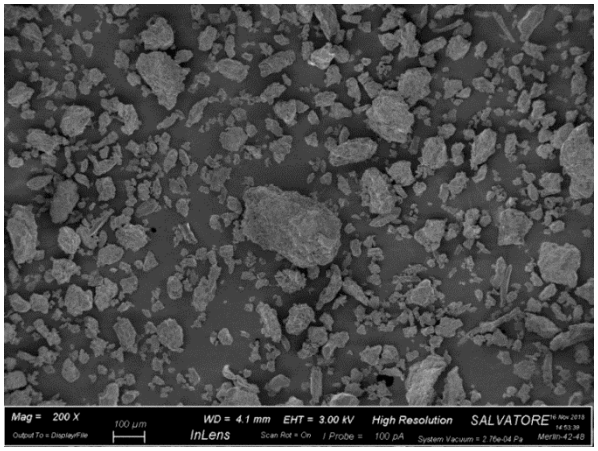

Figure 4.5: SEM image of olive pomace dust sample, 200x magnification

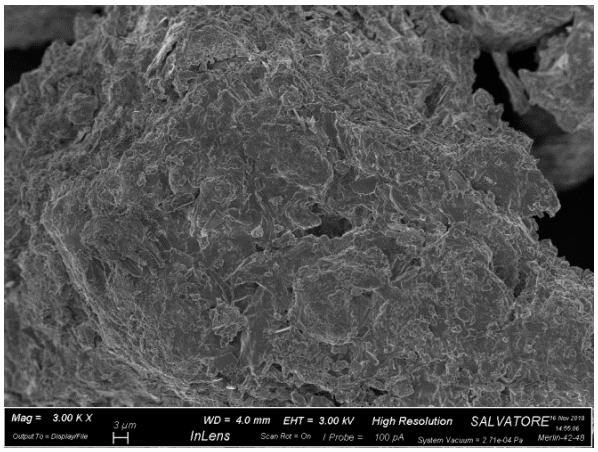

Figure 4.6: SEM image of olive pomace dust sample, 3.00x magnification

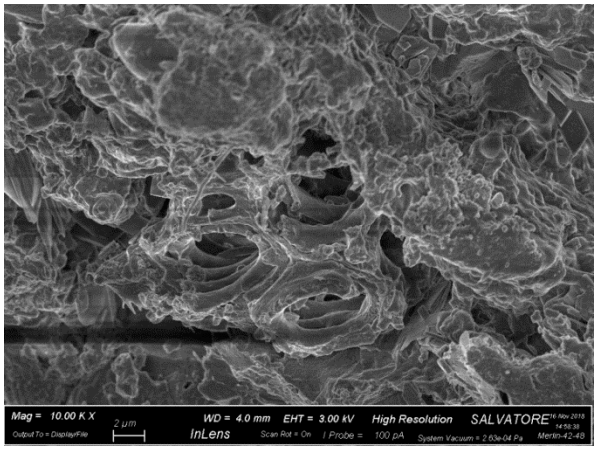

Figure 4.7: SEM image of olive pomace dust sample, 10.00 Kx magnification

4.4 Screening test

The numbers of ignitions or not-ignitions in the screening test with reported for each sample size fraction in table 4.4.

Table 4.4: Results of the tests in the Hartmann tube. N=no ignition, P= ignition, x# indicates the number of ignition or no ignition observed.

		Hartmann tube		***GG furnace***
Sample size[µm]	***Mass [g]***	***Continuous arc***	***Growing wire***	***800˚C***
1000-500	0.3	*x*10 N	*x*10 N	P
	0.5	*x*10 N	*x*10 N	P
	1.0	*x*10 N	*x*10 N	P
< 500	0.3	*x*10 N	*x*10 N	P
	0.5	*x*10 N	*x*10 N	P
	1.0	*x*10 N	*x*10 N	P
< 75	0.3	*x*10 N	*x*10 N	P
	0.5	*x*10 N	*x*10 N	P
	1.0	*x*10 N	*x*10 N	P

The powder was initially tested in the Hartmann tube with a continuous arc. According to the results presented in table No.4.4 the dust samples were not ignited. Therefore, the analysis was carried out with the glowing wire, which has higher ignition energy. Similarly, none of the samples was ignited; this means that the olive pomace dust is not explosive at room temperature.

Due to the negative result in the Hartmann tube tests, the high temperature test was carried out in the GG furnace. All of the samples were ignited. This positive result for ignition in the furnace allowed to classify the olive pomace dust as explosive at high temperatures. Consequently, the screening test in the hot plate was not determined.

4.5 Minimum ignition temperature of a dust cloud (MIT)

The values of minimum ignition temperature (MIT) of the olive pomace dust with size range between 1000-500 µm, <500 µm and <75 µm are reported in table 4.5.

Table 4.5: MIT of olive pomace dust samples.

Dust sample size [µm]	*MIT [˚C]*
1000-500	740
< 500	660
< 250	490
< 75	590

The minimum ignition temperatures (MIT) of the olive pomace dust increased from 590˚C up to 740˚C with increase in particles size analyzed in this study. This behavior is well-known in dust explosion scientific literature and deals with the fact smaller organic particles require a lower amount of energy for the devolatilization compared to the larger ones, as consequence of the specific surface area (Eckhoff R. , 2003). A higher surface area is available for heating transfer and flame propagation. Nonetheless, it is also possible to notice that *<250µm* fractions has the lowest minimum ignition temperature. This does not agree with the trend observed (figure 4.8) in the other sample fractions (<75, <500 and 1000-500µm). This could be attributed to the chemical nature of the olive pomace dust fractions. As explained in section 2.4, olive pomace is a by-product of the extraction process of olive oil, so it is composed mainly of pulp and stones remained in proportion that can vary according to the process and nature of the olive. Additionally, may contain wood remnants of branches and leaves.

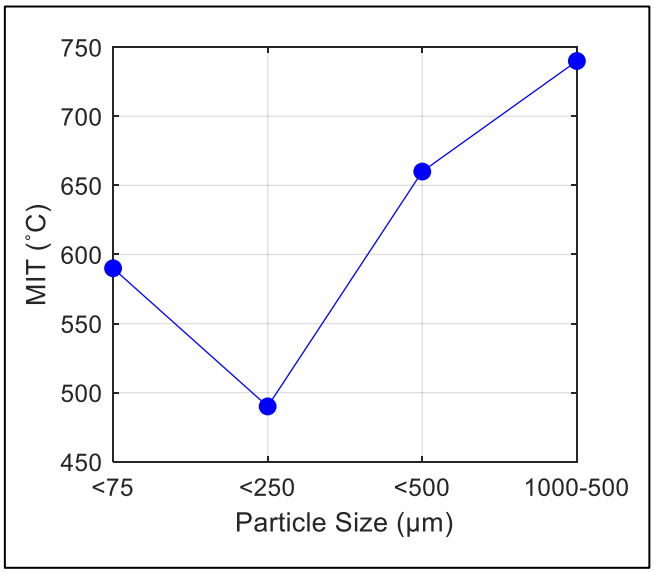

Figure 4.8: Minimum Ignition Temperature of sieve fraction <75, <250, 500-250 and 1000-500µm of the olive pomace dust

4.6 Hot Surface Ignition Temperature of a dust layer

Table 4.6 reports the data acquired in the determination of the minimum ignition temperature of a 5mm dust layer of olive pomace sample with particle size <250µm. Additionally, in Fig. 4.9 the thermokinetic diagrams obtained during the at the temperatures of 280 and 290˚C respectively are shown.

Table 4.6: Results of the tests in the Hot plate device for olive pomace dust <250µm. N=no ignition, P= ignition, x# indicates the number of ignition or no ignition observed.

Temperature [˚C]	*Observation*
250	N
300	P
290	P
280	N x2

According to the data presented in table 4.6, the minimum ignition temperature of the dust layer of olive pomace with particle size <250µm is 290˚C.

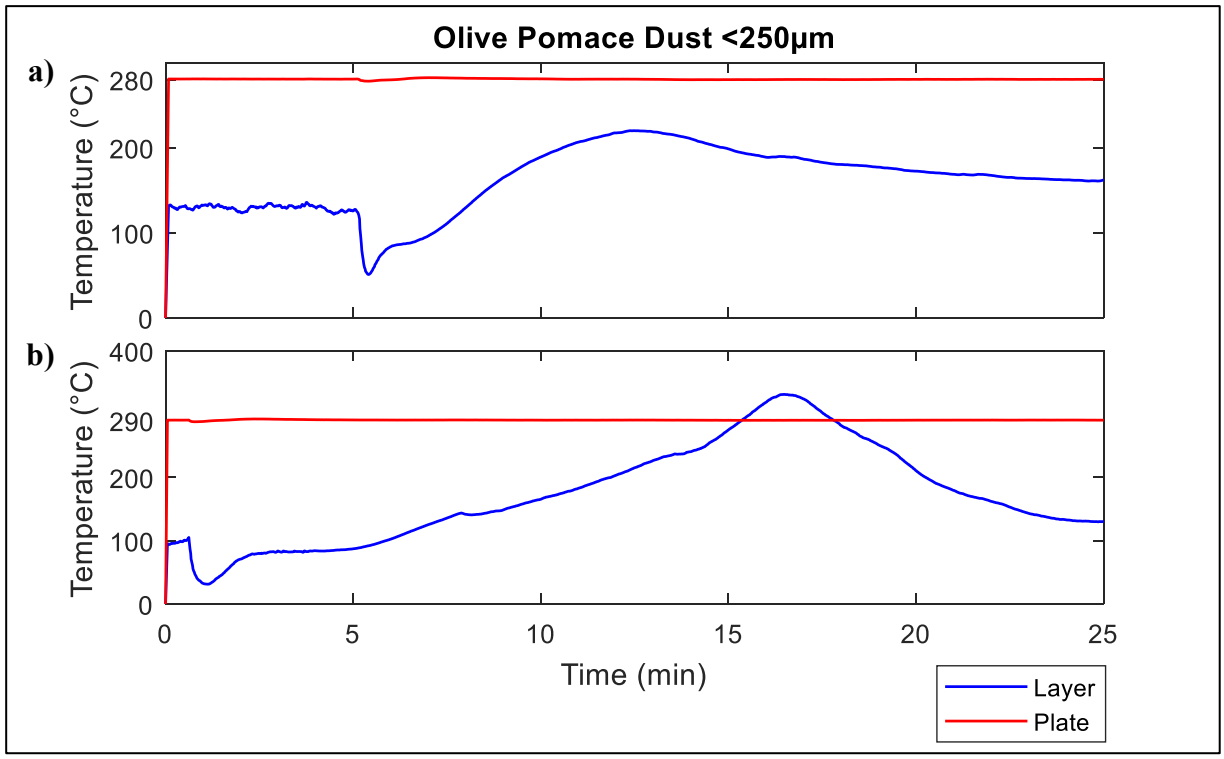

Figure 4.9: Thermokinetic diagrams of the olive pomace dust <250µm, plate temperature: a) 280˚C and b) 290˚C

Initially, the temperature decreases because the sample of dust was added at room temperature on the plate with set temperature. Subsequently, the temperature begins to increase, in this period the evaporation of water occurs as well as the volatilization of other substances present in the olive pomace sample. The curve reaches a maximum, which is greater than the

temperature of the plate in the case of the LIT curve at 290˚C, as a result of the heat generated after the ignition. Finally, the temperature of the dust layer decreases and stabilizes, as no more material is available to the combustion, and air is flowing, through the burnt material, cooling it down.

In figure 4.10, images of the powder layer during the test at 280 C without ignition and the dust layer with the embers at 290˚C.are shown.

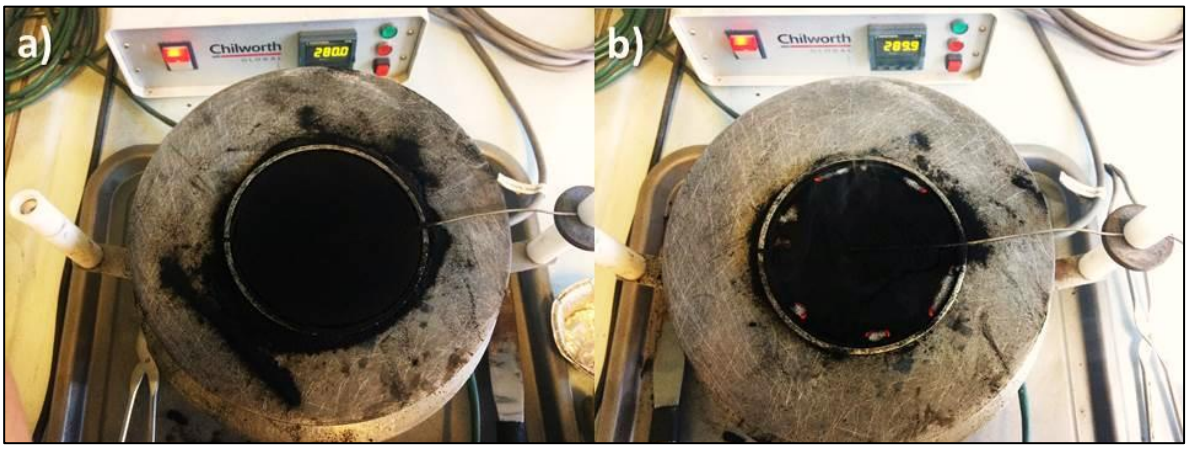

Figure 4.10: *Layer of olive pomace dust <250μm in the hot plate test: a) at 280˚C not ignition and b) at 290˚C ignition.*

4.7 Explosibility parameters- 20 l sphere

The dust samples with dimensions between 500μm and less than 250μm were submitted to explosion tests in the 20 l sphere, in order to quantify the deflagrating parameter K_{st}, P_{max} and LEL.

The evolution of (dP / dt) and Pm as a function of the concentrations for each series of measurements made are illustrated in figures 4.11 and 4.12. The explosibility data obtained are given in table 4.7.

Table 4.7: Explosibility parameters for the olive pomace dust samples.

Dust sample [μm]	K_{St} *[bar m/s]*	P_{max} *[bar]*	$(dP/dt)_{max}$ *[bar/s]*	*LEL [g/ m³]*	*St class*
500-250	21.4	5.9	78.8	> 1250	1
< 250	49.4	6.8	182.1	200	1

It was determined that the olive pomace powder belongs to the St1 class (weak explosion). The K_{st} value obtained for the sample with dimensions less than 250μm is in accordance with that presented in the online database of the Institute for Occupational Safety and Health of the Social Accident Insurance database of Germany (IFA), for olive pellets.

On the other hand, as expected, for the sample with dimensions between 500-250, lower K_{st} and P_{max} values were obtained. According to what is explained in Chapter 2, particles with smaller dimensions lead to more severe explosions, because these particles have a large surface area that increases combustion rate and volatilization.

Besides, from the test conducted with 2*1 kJ igniters, it was confirmed that not overdriving had occurred and the LEL was determined (not for the 500-250μm sample).

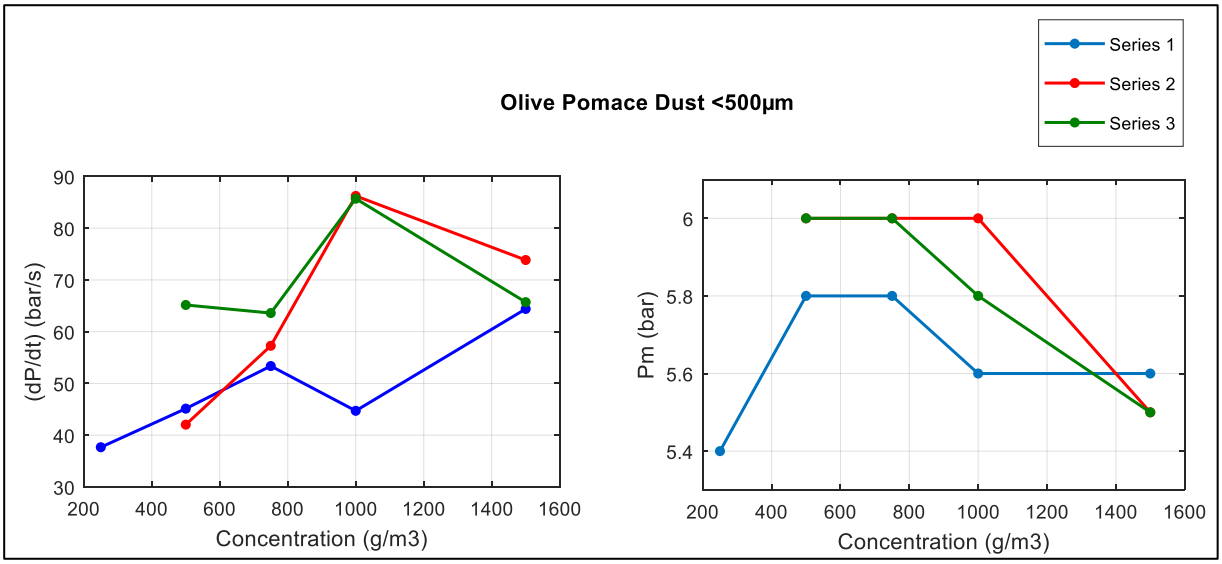

Figure 4.10: Series values for the olive pomace dust size <250µm of the rate of pressure rise and explosion and pressure explosion as a function of dust concentration

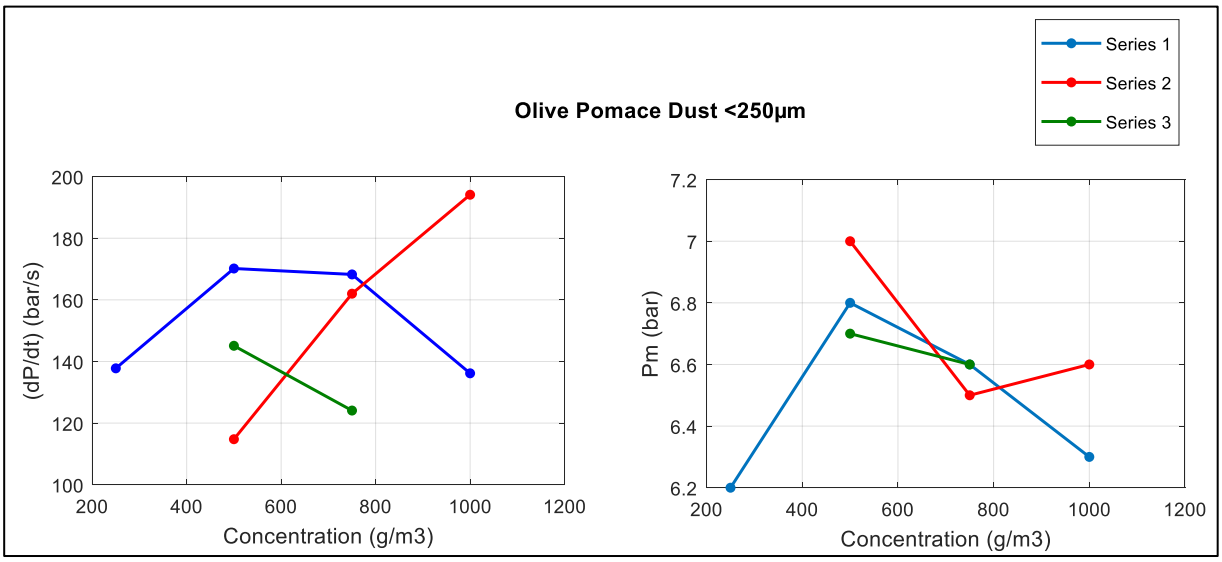

Figure 4.11: Series values for the olive pomace dust size <250µm of the rate of pressure rise and explosion and pressure explosion as a function of dust concentration.

In the figure 4.13 and 4.14 are represented the values of the maximum explosion overpressure Pm and the maximum rate of explosion pressure rise $(dP/dt)_{max}$ obtained in the determination of the LEL.

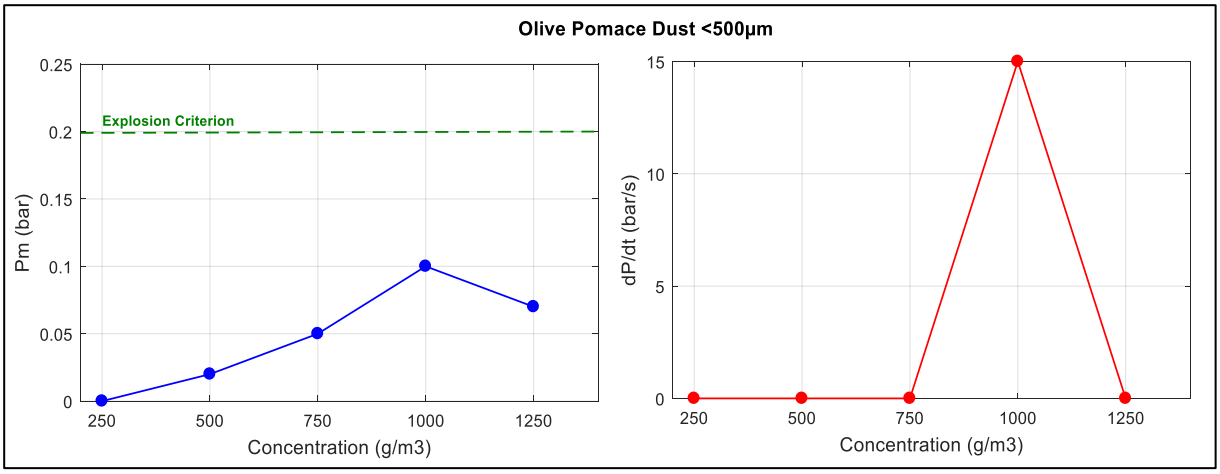

Figure 4.12: Variation of the Pmax and (dP / dt) with concentrations in the LEL measurement for olive powder particles with a size <500µm

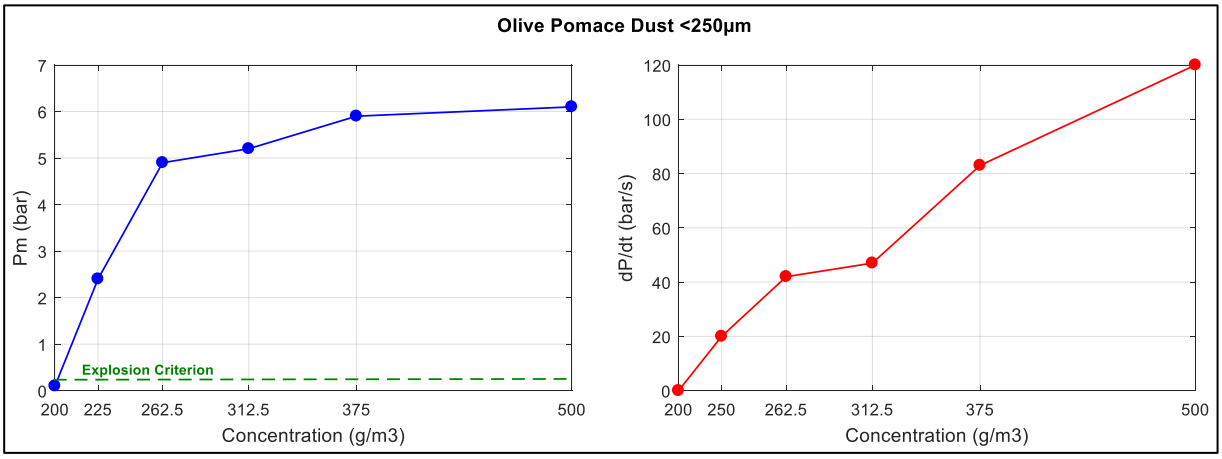

Figure 4.13: Variation of the Pmax and (dP / dt) with concentrations in the LEL measurement for olive powder particles with a size <250µm

According to the normative EN 14034-3 (2006+A1:2011), the concentration in which an explosion is not evidenced defines the LEL. Based on the value of the measured explosion pressure, the criterion described in section 3.6.2.2 was adopted.

The results of the lower explosibility limits (LEL) indicate that no explosions occur up to concentration of olive pomace dust greater than 1250g/m^3 for particles with sizes between 500 and 250µm (greater concentraton were not tested, since issues with the valve inlet could occur with excessive amount of dust), while for particles below 250µm, LEL was found at a concentration of 200 g/m^3.

4.8 Influence of moisture content

To expand the explosive characterization of the olive pomace, Pietraccini M.(2019) determined the minimum ignition temperature (MIT) using a BAM oven, the lower limit of explosivity (LEL) and the explosive parameters (P_{max}, (dP / dt) max and K_{St}) were measurement in the 20l sphere. However, previously the moisture content was reduced below 5% w/w of the same sample used in the present work. To dry the dust, the sample was placed in an air oven at 110 ° C for 24 h. The sample was milled in a hammer mill TM. Despite the

fractions that were subjected to the tests have different particle sizes; it is possible to establish some contrasts between the two research works.

Comparing the results obtained in both studies, it is possible to affirm that when the moisture content is lower, the explosion parameters P_{max}, dP / dt max and K_{St} increase. On the other hand, the minimum ignition temperature of the different fractions decreases.

In Pietraccini's work a lower concentration of olive pomace dust is required to trigger the explosion (LEL) respect to the powder used in this work. This could be explained due to the a higher moisture content in the samples used for this test (no drying dust sample). It can be explained considering that the heating and evaporation of the water act as a heat sink/consume, attenuating the explosive character of the sample.

It is important to bear in mind that the differences between the LEL values of both works are also due to the dried olive pomace in Pietraccini's work was tested following the American ASTM E1515-07 standard instead of the EN 14034-3 (2006) . The American ASTM E1515-07 considers single chemical igniter of 2.5kJ. While European normative establishes that for the measurement of the LEL, two chemical igniters of 1kJ should be used, therefore the total ignition energy used in the test was 2 kJ. In addition, the disposition of chemical igniters inside the sphere in the American standard is different than the one established in the European standard.

5 Conclusions

The explosiveness of olive pomace powder resulting from the extraction of olive oil has been studied in this work. This by-product is mainly composed of stones and pulp of the processed olives, with combustion heat values between 4500-4600 kcal / kg.

The following conclusions can be drawn from this work:

- The olive pomace grinding process has a significant influence on the morphology and particle size distribution.
- The results of the screening test allowed classifying the olive-pomace dust as an "explosive at high temperatures".
- The particle size increases the minimum ignition temperature of a dust cloud. However, the chemical nature of the olive pomace powder influences this temperature values. The different particle sizes have MIT compressed between 490˚C and 740˚C.
- The minimum ignition temperature of a layer of olive-pomace powder with particle size <250μm is equal to 290˚C.
- The results of the tests carried out in the sphere of 20l classify the olive pomace powder as belonging to the class ST1 (K_{St} equal to 21.4 and 49.4 bar m / s respectively for the fractions 500 <d <250 and <250μm. The K_{St} and the maximum explosion pressure increase as the particle size decreases.
- The lower explosive limit LEL decreases with the reduction of the particle size. The particles with a size between 500-250 μm did not trigger for concentration values up to 1250 g / m^3, while the particles below 250μm exhibit an LEL equal to 200 g / m^3.
- The moisture content also has an influence on deflating parameters. Olive pomace powders with significant moisture content have a higher minimum ignition temperature and a lower explosive limit. The moisture content reduces the explosive parameters P_{max} and K_{St}.

6 References

(n.d.). Retrieved from Institute for Occupational Safety and Health of the German Social Accident Insurance : http://staubex.ifa.dguv.de/explokomp.aspx?nr=3152&lang=e

NFPA 68. (2007). *Standard on Explosion Protection by Defragrating Venting*.

A., R., M.L., C., & M.A., S.-M. (2006). An overview on olive mill wastes and ther valorisation methods. *Waste Management*, 20: 960-969.

Abbasi, T., & Abbasi, S. (2007). Dust explosions- cases, causes, consequences, and control. *Science Direct*, 23.

Abu-Qudais, M. (1996). Fluidized-bed combustion for energy production from olive cake. *Energy* , Vol. 21, No.3: 173-178.

Al-Ketan, O. (2012). Potential of using olive pomace as a source of renewable energy for electricity generation in the Kingdom of Jordan. *Journal of Renewable and Sustainable Energy* .

Alkhamis, T. M., & Kablan, M. M. (1999). Olive cake as an energy source and catalyst for oil shale production of energy and its impact on the environment. *Energy Convers*, 77: 97-100.

Amyotte, P. (2013). *An Introduction to Dust Explosions. Understanding the Myths and Realities of Dust Explosions for a Safer Workplace.* Oxford : Butterworth-Heinemann.

Anon. (2000). Improvements of Treatments and Validation of the Liquid-Solid Waste from the Two Phase Olive Oil Extraction. *FAIR CT96 1420*, Annex A2 Final Report Project Improlive.

Arjona, R., Garcia, A., & Ollero, P. (1999). The drying of alpeorujo, a waste product of the olive oil mill industry. *Journal of Food Engineering*, 229-234.

ASTM E1491-06. (2019). *Standard Test Method for Minimum Autoignition Temperature of Dust Clouds*.

ASTM E2021-09. (2013). *Standard Test Method for Hot-Surface Ignition Temperature of Dust Layers*.

Bartknecht, W. (1971). *"Brenngas-und Staubexplosionen." Forschungsbericht F45.* Koblenz: Fedeeral Republic of Germany: Bundesinstitut fur Arbeitsschutz.

Bartknecht, W. (1978). *Explosionen-Ablauf und Schutzmassnahmen.* Berlin: Springer-Verlag.

Barton, J. (2002). *Dust Explosion prevention and protection: a practical guide.* Woburn (Massachusetts): Gulf Publishing Company.

Cashdollar, K. L. (2000). Overview of dust explosibility characteristics. *Journal of Loss Prevention in the Process Industries*, 183-199.

CEI EN50281-2-1. (1999). *Costruzioni elettriche destinate all'uso in ambienti con presenza di polvere combustibile*.

Cesana, C., G., K. A., & Siwek, R. (2016). *20-l-Apparatus KSEP 7.0 Manual.* Bettingen: FireEx Consultant Ltd.

Dastidar, A. G., Amyotte, P. R., & Pegg, M. J. (1997). Factors influencing the suppression of coal dust explosions. *Fuel*, 663-670.

Di, B. A., Di, S. V., & P., R. (2010). On the determination of the minimum ignition temperature for dust/air mixtures. *Chemical Engineering Transactions, 19*.

Doymaz, I., Gorel, O., & Akgun, N. A. (2004). Drying Characteristics of the Solid By-product of Olive Oil Extraction. *Biosystems Engineering*, 88(2), 213–219.

Eckhoff, R. (2003). *Dust Explosions in the Process Industries* . Amsterdam: Gulf Professinal Publishing.

Eckhoff, R. (2016). *Explosion Hazards in the Process Industries* (2nd ed.). Oxfordshire: Gulf Professional Publishing.

Eckhoff, R. K. (2009). Understanding dust explosions. The role of powder science and technology . *Journal of Loss Prevention in the Process Industries*.

EN 13821. (2004). *Potentially explosive atmospheres. Explosion prevention and protection. Determination of minimum ignition energy of dust/air mixtures*.

EN 14034-1. (2004+ A1 2011). *Part 1: Determination of the maximum explosion pressure Pmax of dust clouds*. Brussels.

EN 14034-2. (2006+ A1:2011). *Determination of explosion characteristics of dust clouds. Determination of the maximum rate of explosion pressure rise (dp/dt)max of dust clouds*.

EN 14034-3. (2006+A1:2011). *Determination of explosion characteristics of dust clouds. Determination of the lower explosion limit LEL of dust clouds*.

Fumagalle, A., Derudi, M., Rota, R., & Copelli, S. (2006). Estimation of the deflagration index Kst for dust explosions: A review. *Journal of Loss Prevention in the Process Industries*, 311-322.

G. Nicoletti, F. A. (1999). Bagazo de Oliva. Parte 1: Factibilidad de su uso como combustible alternativo. *Información Tecnológica, 10*, 11-19.

Gummer, J., & Lunn, G. A. (2003). Ignitions of explosive dust clouds by smouldering and flaming agglomerates. *Journal of Loss Prevention in the Process Industries*, 27-32.

Hepbasli, A., Akdeniz, R. C., Vardar-Sukan, F., & Oktay, Z. (2003). Utilization of Olive Cake as a Potential Energy Source in Turkey. *Energy Sources*, 25: 405-417.

Kauffman, C. W. (1982). Agricultural dust explosions in grain handling facilities. *J.H.S. Lee, C.M. Guirao (Eds.)*, 305-347.

Kenneth L. Cashdollar, M. H. (1986). *Industrial Dust Explosions: Symposium on Industrial Dust Explosions.* Pittsburgh: ASTM International.

Kuai, N., Huang, W., Du, B., Yuan, J., Li, Z., Gan, Y., & Tan, J. (2013). Experiment-based investigations on the effect of ignition energy on dust explosion behaviors. *Journal of Loss Prevention in the Process Industries*, 26:869-877.

Lebecki, K., Z. Dyduch, A. F., & Sliz, J. (2003). Ignition of a dust layer by a constant heat flux. *Journal of Loss Prevention in the Process Industries*, 16: 243-248.

Lunn, G. A. (1988). A note on the Lower Explosibility Limit of organic dust. *Journal of Hazardous Materials*, 207-213.

Mendez, P. S., & Ruiz, M. V. (2006). Production of pomace olive oil. *Grasas y Aceites*, 47-55.

NFPA, 6. (2007). *Standard on Explosion Protection by Deflagrating Venting.*

Ogle, R. A. (2016). *Dust Explosion Dynamics.* Warrenville, IL: Butterworth-Heinemann.

Oktay, Z. (2006). Olive Cake as a Biomass Duel for Energy Production. *Energy Sources*, 329-339.

P.R.Amyotte, B.K.Baxter, & M.J.Pegg. (1990). Influence of initial pressure on spark-ignited dust explosions. *Journal of Loss Prevention in the Process Industries*, 261-263.

Pan, L., Ge, B., & Zhang, F. (2017). Indetermination of particle sizing by laser diffraction in the anomalous size ranges. *Journal of Quantitative Spectroscopy & Radiative Transfer*, 20-25.

Petrakis, C. (2006). *Olive Oil* (2nd ed.). Chania: Mediterranean Agronomic Institute of Chania.

Pietraccini, M. (2019). *Explosibility and flammability of four olive pomace dust samples.*

Reay, D. (1977). *User Guide to Fire and Explosion Hazards in Drying of Particulate Materials.* Rugby: Institution of Chemical Engineers.

Retrieved from Institute for Occupational Safety and Health of the German Social Accident Insurance. (n.d.). Retrieved from http://staubex.ifa.dguv.de/explokomp.aspx?nr=3152&lang=e

Skřínský, J. (2017). Influence of pressure and temperature on explosion characteristics of COG/air mixtures measured in 20-L and 1000-L spherical vessels. *WSEAS TRANSACTIONS on ENVIRONMENT and DEVELOPMENT*, 13: 421-430.

UNE. (2007). *Explosive atmospheres- explosion prevention and protection - Part 1: Basic concepts and methodology.*

Yuan, J., Wei, W., Huang, W., Du, B., Liu, L., & Zhu, J. (2014). Experimental investigations on the roles of moisture in coal dust explosion. *Journal of the Taiwan Institute of Chemical Engineers*, 2325-2333.